

See discussions, stats, and author profiles for this publication at: <https://www.researchgate.net/publication/236082520>

Hybrid Lipids Increase the Probability of Fluctuating Nanodomains in Mixed Membranes

ARTICLE *in* LANGMUIR · MARCH 2013

Impact Factor: 4.46 · DOI: 10.1021/la4006168 · Source: PubMed

CITATIONS

20

READS

38

2 AUTHORS, INCLUDING:



Benoit Palmieri

McGill University

21 PUBLICATIONS 412 CITATIONS

SEE PROFILE

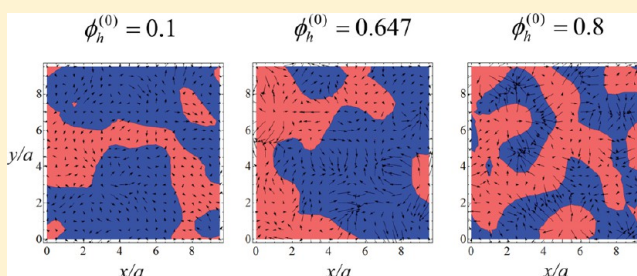
Hybrid Lipids Increase the Probability of Fluctuating Nanodomains in Mixed Membranes

Benoit Palmieri and Samuel A. Safran*

Department of Materials and Interfaces, Weizmann Institute of Science, Rehovot 76100, Israel

S Supporting Information

ABSTRACT: A ternary mixture model is proposed to describe composition fluctuations in mixed membranes composed of saturated, unsaturated, and hybrid lipids (with one saturated and one unsaturated hydrocarbon chain). The hybrids are line-active and can reduce the packing incompatibility between the saturated and unsaturated lipids. We introduce a lattice model that extends previous studies by taking into account the dependence of the interactions of the hybrid lipids on their orientations in a simple way. A methodology to recast the free energy of the lattice model in terms of a continuous, isotropic field theory is proposed and used to analyze composition fluctuations in the one-phase region (above the critical temperature). The effect of hybrid lipids on fluctuation domains rich in saturated/unsaturated lipids is predicted. The correlation length of such fluctuations decreases significantly with increasing amounts of hybrids; this implies that nanoscale fluctuation domains are more probable compared to the case with no hybrids. Smaller correlated fluctuation domains arise even when the temperature is close to a critical point, where very large correlation lengths are normally expected. This decrease in the correlation length is largest as the hybrid composition tends toward a crossover value above which stripelike fluctuations are predicted. This crossover value defines the Lifshitz line. The characteristic wavelength of the stripelike fluctuations is large close to the Lifshitz point but decreases toward a molecular size in a membrane that contains only hybrids. Micrometer size, stripelike domains have recently been observed experimentally in giant unilamellar vesicles (GUVs) made of saturated, unsaturated, and hybrid lipids. These results suggest that the line activity of hybrid lipids in such mixtures may be significant only at large hybrid fractions; in that regime, the interface between domains can be diffuse and several hybrid molecules with correlated orientations can separate saturated and unsaturated lipid regions.



1. INTRODUCTION

Cell membranes are multicomponent mixtures composed of many kinds of lipids, cholesterol, and proteins.^{1,2} It has recently been proposed that the plasma membrane of the cell contains domains of fairly uniform lipid composition whose dimensions are on the order of 10–100 nm, much larger than the size of individual lipid headgroups but much smaller than the overall cell extent.^{3–6} It has also been hypothesized that these lateral heterogeneities of cell membranes, often called lipid rafts, play an important role in many cellular processes.^{7–9}

The heterogeneity of membrane bilayers has been the focus of experimental studies in biological cells (refs 10 and 11 and references therein). In cells, rafts can be explained by effects that are unrelated to the physical interactions of the lipids, including the possibilities that lateral heterogeneities could arise from the coupling between the membrane composition and the cortical cytoskeleton,^{12,13} from the coupling between the membrane curvature and the composition,¹⁴ from cell–cell adhesion,¹⁵ or from the interactions between lipids and proteins.^{16–18}

However, the fundamental and interesting physics related to lipid interactions in these systems are best studied in simpler systems (i.e., model membranes comprising only a few

components). One useful approach measures the properties of giant unilamellar vesicles (GUVs) or suspended bilayers whose lipid composition can either be controlled^{19–25} or extracted directly from cell membranes.^{3,19,26} Their size allows composition heterogeneities to be monitored with techniques that cannot resolve small domains in real cells such as fluorescence and confocal microscopy.

The phase behavior of GUVs with various components has been studied experimentally^{2,22,23,27} and theoretically.^{28–30} The mechanism for nanoscale domain formation in model membranes (where there is no cytoskeleton or cell activity) is still under debate, but it is often described within one of two points of views: they are considered to be either small, stable domains in the phase-separated regime or long-lived fluctuations in the single phase (where all components are uniformly mixed) of the membrane.^{3,31} Such long-lived fluctuations are relevant to the lipid raft hypothesis only if the lifetime of saturated lipid-rich domains that can form in the single phase is long compared to biological processes. The simplest

Received: November 3, 2012

Revised: March 10, 2013

Published: March 26, 2013

description of the membrane, a binary, lipid mixture model, does not obviously account for the emergence of nanoscale domains in either picture. Below the phase-transition temperature, the theory of binary mixtures predicts macroscopically large phase-separated domains and no stable nanodomains. If the temperature is finely tuned above the critical temperature, composition fluctuations can then have characteristic sizes on the order of tens of nanometers. At such temperatures, critical slowing is still significant and the effective diffusion coefficient is about 3 orders of magnitude smaller than the normal lipid diffusion value, $D \approx 2 \mu\text{m}^2/\text{s}$. (See ref 3.) This means that composition fluctuations of $\sim 20 \text{ nm}$ will have a lifetime on the order of 10^{-1} s , which appears to be too short for the saturated lipid-rich domains to be biologically relevant in real cells. This implies that theories for nanoscale domain formation in model membranes that may be relevant to lipid rafts, whether existing as fluctuations in the single phase or as stable, finite domains in the phase-separated state, must go beyond the simple binary mixture model.

It is now clear that more than one mechanism can account for lateral heterogeneities in model membranes, although which one (if any) dominates in real cells is still unknown. In the theory presented in this Article, the membrane is treated as a mixture of saturated lipids (neither hydrocarbon chain has double bonds), unsaturated lipids (both hydrocarbon chains have one double bond), and hybrid lipids (one chain has a double bond and the other has none). Phase separation of saturated and unsaturated lipids occurs because of the packing incompatibility between their hydrocarbon chains; the “bent” unsaturated chains tend to demix from the “straight” saturated ones. The hybrid lipid has one chain of each type, it can act as a linactant (2D analog of a surfactant³²) by assembling at the saturated–unsaturated interface. In that case, the packing incompatibility (i.e. the line tension) between saturated and unsaturated domains is reduced. This is illustrated in Figure 1.

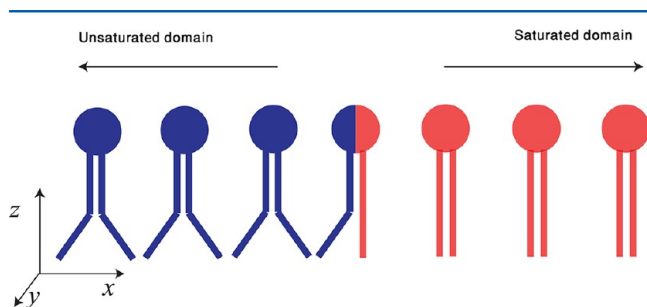


Figure 1. Illustration: The packing incompatibility between domains of saturated (both carbon chains are straight) and unsaturated lipids (both chains are bent) can be reduced when hybrid lipids (one chain is straight and the other is bent) assemble at the interface with the proper orientation. The convention we use here is that unsaturated lipids are blue, saturated lipids are light red, and hybrid lipids have both colors. Also, the normal of the membrane is defined to be in the z direction.

Note that such a ternary mixture is more relevant to model membranes than to real cell membranes that do not contain unsaturated lipids. Hence, in discussing three-component model systems, we shall refer to nanodomains instead of lipid rafts because the latter term is usually associated with real cells.

This possibility for the stabilization of nanodomains was first suggested by Brewster et al.³³ In their original paper, they considered an equilibrium 2D microemulsion with finite

domains of phase-separated saturated and unsaturated lipids where the interfacial energy is reduced by an infinitely small amount of hybrids. Their results showed that the line tension reduction was significant only at relatively low temperatures. For such a membrane where the hybrid component is dilute, a large translational entropy cost must be paid for hybrid lipids to accumulate at the interface. Hence, close to the phase-transition temperature, one might expect that only a relatively small fraction of the hybrid lipids will be at the interface and that the corresponding reduction of the line tension will be small.

The roles of chain order and packing incompatibility were incorporated into this theory by Yamamoto et al., who considered a binary mixture membrane made of saturated and hybrid lipids in the phase-separated regime.^{34,35} In this more microscopic model, the lipid–lipid interactions depended on the local lipid chain order parameter, which had been assumed to be constant in ref 33. For a system containing only hybrid and saturated lipids (relevant to the situation in biological membranes), there is no translational entropy cost for localizing the hybrids to the interface because they are already there. However, there is still an entropic cost related to the order in the hybrid orientation at the interface so that when a hybrid lipid is at the interface its saturated tail points in the energetically favorable direction (toward the saturated domain); it is only this orientation that tends to lower the line tension. This model also predicted a finite but small reduction of the line tension between domains close to the critical temperature.

Following upon these ideas, several other studies reported significant effects of hybrid lipids in membrane bilayers. The molecular dynamics simulations of Schäfer and Marrink demonstrated that hybrid lipids can act as linactants and tend to accumulate at the boundary between domains of saturated and unsaturated lipids.³⁶ The line tension reduction calculated in their particular simulations was significant but not enough to produce finite, equilibrium domains in the phase-separated regime. Experimentally, Szekely et al. performed studies on ternary (saturated–unsaturated–hybrid) mixtures of membrane stacks in the presence of calcium ions. Under the conditions described in ref 37, the system exhibits a multilamellar phase and the spacing between the membranes was probed by X-ray scattering. In a system with only saturated and unsaturated lipids, two distinct intermembrane separation distances were measured; one corresponds to the single-phase state and the other to the phase-separated state. Their results showed that these distances changed in a manner that suggested the mixing of saturated and unsaturated lipids as the fraction of hybrid lipids was increased. Finally, by fluorescently labeling GUVs, keeping the temperature fixed but varying the fraction of hybrid lipids in a membrane mixture (saturated/unsaturated/hybrid lipids and cholesterol), Konyakhina et al. showed that the local membrane structure varied from complete phase separation (in the case of no hybrids) to complete mixing (in the case of a relatively large fraction of hybrids) with intermediate modulated phases;²⁴ however, those modulations were in the micrometer range and not nanoscopic.

In this Article, we present a model that captures the linactant property of hybrid lipids in two ways that are important to describing the line-active ability of hybrid lipids. First, our theory extends the model of Brewster et al. applicable to a ternary mixture of saturated, unsaturated, and a very dilute amount of hybrid lipids to systems with arbitrary hybrid composition, including the case of pure hybrid membranes.

Because the hybrid component is not dilute, the translational entropy cost that diminishes the line tension reduction by the hybrid lipids is mitigated. Second, we propose a model for the orientation interactions involving hybrid lipids, a component of the physics that was neglected when only the dilute limit was considered. This effect further lowers the interaction energies of hybrids lying at the interface and thereby competes with the above-mentioned orientation entropic cost to enhance their line activity.

We first introduce a microscopic lattice model that accounts for these two extensions of the theory. Next, we show how to transform the lattice model into a rotationally invariant, Landau–Ginzburg type of field theory, such as the one proposed in ref 38 to describe microemulsions. In our theory, the behavior of the system depends on only one interaction energy parameter whose value is fully specified by the transition temperature. The effect of hybrid lipids on the composition fluctuations in the single-phase regime where all components are macroscopically mixed is predicted. We note that in principle the same theory also applies to the phase-separated regime. However, our interest here is to connect our model to the experiments of Veatch et al.,^{3,31} which suggest that biological rafts are a manifestation of nearly critical composition fluctuations in the one-phase region. In most mixtures, the correlation length associated with the critical fluctuation is very large when the temperature is close to the critical point. We will demonstrate that this is not necessarily the case in the mixed membrane considered here because the line activity of the hybrid lipids can significantly reduce the correlation length, even if the temperature is maintained relatively close to the critical point.

Another recent theoretical study³⁹ has also discussed the effects of hybrid lipids on composition fluctuations. In that work, Hirose, Komura, and Andelman proposed a phenomenological free energy to describe a membrane with saturated and hybrid lipids. The main difference between our work and theirs lies in the modeling of the free energy. Our proposed orientationally dependent microscopic interactions give rise to a free energy whose dependence on the hybrid orientation degrees of freedom differs qualitatively from the one proposed in ref 39. This difference becomes more important as the hybrid lipid fraction is increased. In addition, because all of the interactions in our microscopic model originate in the chain-packing incompatibility that is the same (per chain type) for all of the lipids, we have only one interaction energy parameter; the phenomenological approach proposed by Hirose et al.³⁹ has six parameters.

The Article is organized as follows. In section 2, we present our lattice model for the ternary membrane and specify the microscopic interactions. In section 3, we use standard statistical mechanics principles to derive an expression for the local free energy of the system that allows us to predict the composition correlation functions that can be measured with scattering. The variational principle that we use to calculate the free energy is described in section 3.1. In section 3.2, we show how the lattice free energy can be recast as an isotropic field theory that is independent of any underlying lattice. Section 4 presents our results. The model free energy is first used to define the spinodal (the temperature above which all fluctuations, both macroscopic and those with finite wave-vectors, are locally stable but could be preempted by first-order transitions) and the critical temperature of the mixed membrane. In section 4.1, correlation functions of composition

fluctuations in the membrane are predicted as a function of the hybrid lipid composition. For the picture in which nanoscale domains are viewed as composition fluctuations, such correlation functions predict the effect of hybrid lipids on the nanodomain length scale. Sections 4.2 and 4.3 report orientation correlation functions and the average composition near a hybrid lipid with a fixed orientation. This illustrates how hybrid lipids cooperate with neighboring molecules. Section 5 contains the discussion and some concluding remarks. We conclude the introduction with advice directed to readers less interested in the more technical aspects of our work; it is probably enough for them to focus on section 2 (to understand the set of microscopic interactions), section 4 until the end of section 4.1 (our main result), and the Discussion.

2. LATTICE MODEL

This section presents our lattice model representation of one of the bilayer leaflets in a three-component (saturated–unsaturated–hybrid) mixed-lipid membrane. We show below how this can be translated into a continuum model so that the details of the lattice are no longer important. It is well known that the two leaves of a bilayer have some degree of correlation³⁹ but recent experiments reported only small couplings between the membrane order of the two leaflets (however, the lateral lipid diffusion was coupled).⁴⁰ Here we will focus on one leaflet because internal couplings within a single leaf can lead to domains. For simplicity, the lipids are placed on a square lattice where each site is occupied by one type of lipid (Figure 2A).

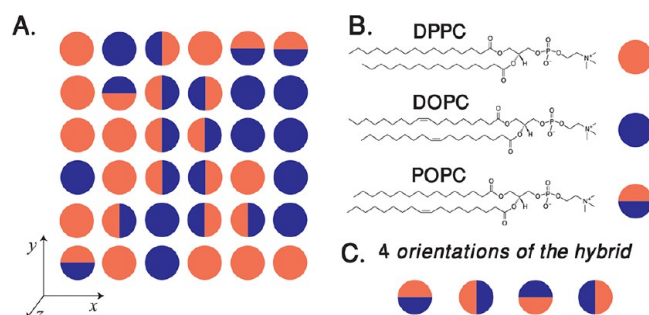


Figure 2. (A) Top view of a section of the membrane modeled as a square lattice. Each site can be occupied by a saturated lipid (light red circle), an unsaturated lipid (blue circle), or a hybrid lipid (light red/blue circle). (B) Example of saturated, unsaturated, and hybrid lipids. They are, respectively, DPPC (1,2-dipalmitoyl-*sn*-glycero-3-phosphocholine), DOPC (1,2-dioleoyl-*sn*-glycero-3-phosphocholine), and POPC (1-palmitoyl-2-oleoyl-*sn*-glycero-3-phosphocholine). (C) Each hybrid lipid can assume one of the four orientations shown.

Curvature effects were recently proposed as a mechanism for the formation of modulated phases⁴¹ and microemulsions¹⁴ in bilayers. Here, the 3D curvature of the membrane is not taken into account; we consider systems where the coupling between the composition and the curvature is small. In the system that we consider, phase separation is driven by the packing incompatibility of the saturated/unsaturated hydrocarbon chains. A difference in the polar headgroup (charge, size) can also lead to phase separation,^{42,43} but we focus here on the role of the chains because that is what primarily distinguishes the saturated, unsaturated, and hybrid lipids. We thus assume that the headgroups of all three lipids are identical. As shown below, this allows us to parametrize the interactions with one effective interaction constant. Figure 2B shows the chemical structure of

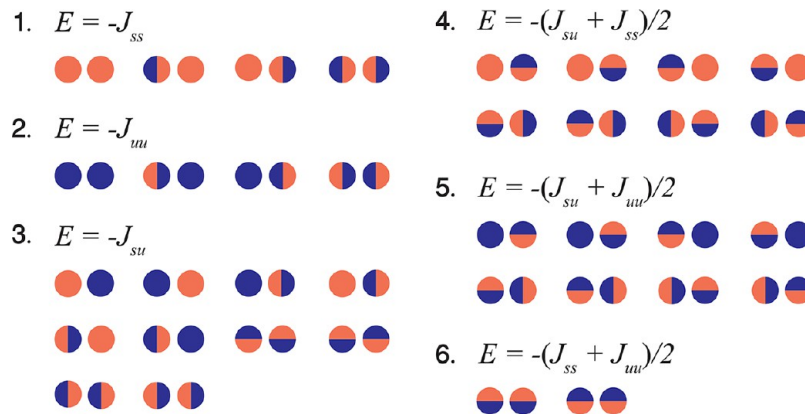


Figure 3. All possible nearest-neighbor configurations and their interactions energies. For each of the 36 possible types of pairs, we assign 1 of 6 interaction energies. The packing energies are determined by the interactions between nearest chains (J_{ss} , J_{uu} , and J_{su}) on two neighboring lipids. Each of the six panels is discussed in the main text.

typical lipids that could be described by our model: DPPC (saturated), DOPC (unsaturated), and POPC (hybrid). The GUVs and the membrane stacks studied in refs 24 and 37 comprised these types of lipids.

The lattice model is inspired by previous ones that describe the self-assembly of amphiphilic systems^{44,45} in three dimensions and is a special case of the model discussed by Matsen and Sullivan.⁴⁶ The hybrid lipid is asymmetric, so its orientation in the plane of the membrane must be taken into account. Here, we model these orientation degrees of freedom by allowing the hybrid to have one of the four orientations shown in Figure 2C. The following description of the nearest-neighbor interactions is based on the degree of packing compatibility between hydrocarbon chains.^{34,47} As in the work of Brewster et al.,³³ the packing energy of a pair of nearest-neighbor lipids is denoted as $-J_{ss}$, $-J_{uu}$, and $-J_{su}$ if the closest two chains, each belonging to a different lipid molecule in the interacting pair, are respectively both saturated, both unsaturated, and one is saturated and the other is unsaturated. In a binary mixture of saturated and unsaturated lipids, phase separation can occur if $J_{ss} + J_{uu} - 2J_{su} > 0$; the packing incompatibility between the saturated and unsaturated hydrocarbon chains favors the aggregation of lipids of the same type and results in macroscopic domains at low enough temperatures.

A complete description of the interaction energies used in our model is given in Figure 3. Note that all possible interactions are given in terms of J_{ss} , J_{uu} , and J_{su} . This allows us to assign 1 of 6 possible energies to each of the 36 possible nearest-neighbor configurations. In the four configurations shown in panel 1 of Figure 3, a saturated tail faces another saturated tail. Hence the energy of the pair is $-J_{ss}$. In panel 2, the energy of the pair is $-J_{uu}$; an unsaturated tail faces another unsaturated tail. In panel 3, the energy of the pair is $-J_{su}$; a saturated tail faces an unsaturated tail. In panel 4, the energy of the pair is $-(J_{su} + J_{ss})/2$. The pair involves at least one hybrid lipid whose orientation is such that the saturated tail of its neighbor (saturated or hybrid lipid) faces “half” of its saturated tail and “half” of its unsaturated tail. In panel 5, a similar argument determines the energy of the pair to be $-(J_{su} + J_{uu})/2$. Finally, panel 6 shows a configuration having an energy equal to $-(J_{ss} + J_{uu})/2$. Two hybrid lipids are nearest-neighbors. They have the same orientation, which points along the direction perpendicular to their separation vector. In this configuration,

the saturated tails of both hybrids are close together and so are their unsaturated tails.

This model differs from that of Brewster et al. by the fact that we account not only for hybrid interactions with the two other types of lipids but also consider hybrid–hybrid interactions. In ref 33, the hybrid lipids were assumed to be dilute and their mutual interactions were neglected. They assembled at the interface between saturated and unsaturated lipid domains with only one orientation—the one that reduces the packing incompatibility (Figure 1). The current model relaxes all of these limitations. Hybrid lipids interact with each other, both in the bulk and when they lie at the interface. Their interactions, either involving another neighboring hybrid lipid or a fully saturated/unsaturated lipid, are orientationally dependent, and the four orientations depicted in Figure 2C are allowed. The mutual interactions of the hybrids favor their assembly (at saturated–unsaturated interfaces and in the bulk), compared to previous theories. Note that the microscopic interactions used in the lattice model could be refined in many ways. However, one major purpose of this work is to account for the orientationally dependent interactions of the hybrid lipids, which the model captures in a very simple way.

3. FREE ENERGY

The free energy of the system, F' , is obtained from the partition function that is given by

$$Z = e^{-F'/T} = \prod_{i,j} \sum_{\{S_{ij}\}} \sum_{\{n_{ij}\}} e^{-[E(S^s, S^u, S^h, n_x, n_y) - \sum_{ij} (\mu_s^s S_{ij}^s + \mu_u^u S_{ij}^u + \mu_h^h S_{ij}^h)]/T} \quad (1)$$

where

$$\sum_{\{S_{ij}\}} = \sum_{S_{ij}^s=0}^1 \sum_{S_{ij}^u=0}^1 \sum_{S_{ij}^h=0}^1 \delta_{1, S_{ij}^s + S_{ij}^u + S_{ij}^h} \quad \text{and} \\ \sum_{\{n_{ij}\}} = \sum_{n_{x,ij}=-S_{ij}^h}^{S_{ij}^h} \sum_{n_{y,ij}=-S_{ij}^h}^{S_{ij}^h} \delta_{S_{ij}^h, n_{x,ij}^2 + n_{y,ij}^2} \quad (2)$$

where S_{ij}^s , S_{ij}^u , and S_{ij}^h are, respectively, equal to 1 if a saturated, unsaturated, and hybrid lipid occupies the 2D lattice site whose indices are denoted by ij and zero otherwise. The Kronecker delta function $\delta_{1, S_{ij}^s + S_{ij}^u + S_{ij}^h}$ forces all sites to be occupied by one

and only one type of lipid. If there is a hybrid lipid at site ij , then it has a choice of four orientations determined by the values of $n_{x,ij}$ and $n_{y,ij}$ and enforced by the Kronecker delta function, $\delta_{n_{x,ij}^2 + n_{y,ij}^2}$. Respectively, from left to right in Figure 2C, $n_x = 0$ and $n_y = -1$, $n_x = 1$ and $n_y = 0$, $n_x = 0$ and $n_y = 1$, and finally $n_x = -1$ and $n_y = 0$. Note that the factor of S_{ij}^h that appears in this last delta function accounts for the fact that saturated and unsaturated lipids that have identical tails do not have orientation degrees of freedom. The sum over states requires that all sites ij of the 2D lattice be summed over these six possible types of occupation. This is taken into account by the product over all values of ij . A given state is weighted by the Boltzmann factor $\exp[-E(S^s, S^u, S^h, n_x, n_y)/T - \sum_{ij}(\mu_s S_{ij}^s + \mu_u S_{ij}^u + \mu_h S_{ij}^h)/T]$, where $E(S^s, S^u, S^h, n_x, n_y)$, the energy of the configuration, is obtained by summing over the energies of all nearest-neighbor pairs in the lattice. The energy of each pair corresponds to one of the cases described in Figure 3, and a lattice sum expression for $E(S^s, S^u, S^h, n_x, n_y)$ is given by eq S11 in the Supporting Information. Chemical potentials μ_s , μ_u , and μ_h respectively account for the fact that the average membrane composition of the saturated, unsaturated, and hybrid lipids is constrained by the experimental preparation of the bilayer. Finally, T is the temperature measured in units of energy (multiplied by the Boltzmann constant k_B), and F' is the constrained free energy.

3.1. Free Energy in the One-Phase Region: Variational Principle. The partition function written above cannot be evaluated analytically, hence we use a variational approach to obtain the lowest possible upper bound for the system free energy⁴⁸ within a given approximation scheme. We use a reference energy functional, $E_0(S^s, S^u, S^h, n_x, n_y)$, for which an analytical expression for the partition function can be obtained. The Gibbs–Bogoliubov–Jensen–Peierls inequality can then be used to show that

$$F \leq F_0 + \langle E(S^s, S^u, S^h, n_x, n_y) - E_0(S^s, S^u, S^h, n_x, n_y) \rangle_0 \quad (3)$$

where F_0 is the reference free energy, $\langle \dots \rangle_0$ is an average taken with respect to the reference energy functional, and where the constraints imposed by the chemical potentials have been absorbed in the free energy F (F is a Legendre transform of F'),

$$F = F' + \langle \sum_{ij} (\mu_s S_{ij}^s + \mu_u S_{ij}^u + \mu_h S_{ij}^h) \rangle_0 \quad (4)$$

Below, we use this theorem to obtain an approximation for the local free energy of the system; the local (as opposed to global, macroscopic) free energy is required so that we can calculate fluctuations and correlation functions within our approximation scheme.

The following form for E_0 ,

$$\begin{aligned} E_0(S^s, S^u, S^h, n_x, n_y) \\ = T \sum_{ij} (\beta_{s,ij} S_{ij}^s + \beta_{u,ij} S_{ij}^u + \beta_{h,ij} S_{ij}^h + \beta_{x,ij} n_{x,ij} + \beta_{y,ij} n_{y,ij}) \end{aligned} \quad (5)$$

is linear in S^s, S^u, S^h, n_x, n_y , so the partition function and other properties can easily be evaluated. The lowest upper bound for the free energy can then be obtained by minimizing eq 3 with respect to the reference energy parameters $\beta_s, \beta_u, \beta_h, \beta_x$, and β_y or, equivalently, with respect to the average local compositions

and orientation of the hybrid obtained with the reference energy,

$$\phi_{s,ij} = \langle S_{ij}^s \rangle_0, \phi_{u,ij} = \langle S_{ij}^u \rangle_0, \sigma_{x,ij} = \langle n_{x,ij} \rangle_0, \sigma_{y,ij} = \langle n_{y,ij} \rangle_0 \quad (6)$$

and where $\phi_{h,ij} = 1 - \phi_{s,ij} - \phi_{u,ij} = \langle S_{ij}^h \rangle_0$.

Technical details of this local variational approximation are given in the Supporting Information. In summary, we have defined,

$$\begin{aligned} \mathcal{F} \equiv \mathcal{E} - TS \equiv F_0 \\ + \langle E(S^s, S^u, S^h, n_x, n_y) - E_0(S^s, S^u, S^h, n_x, n_y) \rangle_0 \end{aligned} \quad (7)$$

which is the upper bound for F . \mathcal{E} is the energy part of the upper bound and is given by

$$\begin{aligned} \mathcal{E} \equiv -J \sum_{ij} \{ \Psi_{ij}(\Psi_{i+1j} + \Psi_{ij+1}) + \Psi_{ij}\sigma_{x,i+1j} - \sigma_{x,ij}\Psi_{i+1j} \\ + \Psi_{ij}\sigma_{y,ij+1} - \sigma_{y,ij}\Psi_{ij+1} - \sigma_{x,ij}\sigma_{x,i+1j} + \sigma_{x,ij}\sigma_{x,ij+1} \\ - \sigma_{y,ij}\sigma_{y,ij+1} + \sigma_{y,ij}\sigma_{y,i+1j} \} \end{aligned} \quad (8)$$

where

$$J = \frac{1}{2} \left(\frac{J_{ss} + J_{uu}}{2} - J_{su} \right) \quad (9)$$

is the single, effective interaction energy parameter and where the local composition difference is

$$\Psi_{ij} = \phi_{s,ij} - \phi_{u,ij} \quad (10)$$

The full expression for the entropic part of \mathcal{F} is given by eq S9 in the Supporting Information. We are interested in small, local deviations of the equilibrium state composition above the transition temperature (i.e., in the single-phase regime) where the composition is uniform throughout the membrane and the mean orientation vanishes. Hence, the entropic part of the free energy is expanded to second order in small fluctuations about the average compositions and orientations,

$$\begin{aligned} -S \equiv - \sum_{ij} \left\{ \phi_s^{(0)} \log \phi_s^{(0)} + \phi_u^{(0)} \log \phi_u^{(0)} + (1 - \phi_s^{(0)} - \phi_u^{(0)}) \right. \\ \log(1 - \phi_s^{(0)} - \phi_u^{(0)}) + \frac{(\phi_{s,ij} - \phi_s^{(0)})^2}{2\phi_s^{(0)}} + \frac{(\phi_{u,ij} - \phi_u^{(0)})^2}{2\phi_u^{(0)}} \\ \left. + \frac{(\phi_{h,ij} - \phi_h^{(0)})^2}{2\phi_h^{(0)}} + \frac{\sigma_{x,ij}^2 + \sigma_{y,ij}^2}{\phi_h^{(0)}} \right\} \end{aligned} \quad (11)$$

where the superscript (0) indicates the average membrane composition. As discussed above, average compositions are constrained by the experimental preparation of the bilayer, which is why all linear terms in the free energy are canceled by the corresponding chemical potentials. We therefore omitted them in eq 11. Note that the constant terms in the same equation describe the mean field, entropic contribution to the free energy of a ternary mixture.

Before going further, we analyze our expression for the energy derived from the lattice model and given by eq 8. The energy terms each contain the same factor of J that accounts for the interactions between neighboring lipids. Note that J is the only system parameter that, as we will see below, is completely

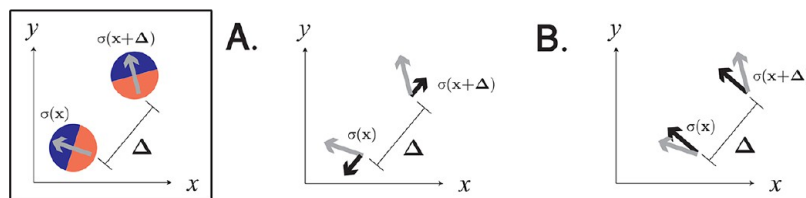


Figure 4. Illustration of orientation–orientation interactions that enter the energy expression in the isotropic theory (eq 15). The gray arrows represent the orientations of neighboring hybrids (also shown in the left panel). (A) The black arrows represent the projection of the orientation components parallel to their separation vector (relevant to the term $[\hat{\Delta} \cdot \bar{\sigma}(\mathbf{x})][\hat{\Delta} \cdot \bar{\sigma}(\mathbf{x} + \bar{\Delta})]$ in eq 15). (B) The black arrows represent the projection of the orientation components perpendicular to their separation vector (relevant to the term $[\hat{\Delta} \times \bar{\sigma}(\mathbf{x})] \cdot [\hat{\Delta} \times \bar{\sigma}(\mathbf{x} + \bar{\Delta})]$ in eq 15).

determined by the transition (demixing) temperature. The first term in the energy expression (eq 8) is $-\Psi_{ij}(\Psi_{i+1j} + \Psi_{ij+1})$. It favors (is negative for) large uniform fluctuations in the one-phase region; these fluctuations are characterized by regions in which either saturated lipids are surrounded by neighboring saturated lipids or unsaturated lipids are surrounded by neighboring unsaturated lipids. The following term in the energy, $-\Psi_{ij}\sigma_{x,i+1j}$, comes from the orientation dependence of the interaction of the hybrid lipids with the saturated/unsaturated lipids. If site ij is occupied by a saturated lipid ($\Psi_{ij} > 0$), then our model suggests that it is energetically favorable to have a hybrid lipid at $i + 1j$ whose saturated tail points to the left such that $\sigma_{x,i+1j} > 0$ (this scenario is described by the second hybrid lipid orientation from the left in Figure 2C). This is the case because this configuration results in an overall negative sign for the term $-\Psi_{ij}\sigma_{x,i+1j}$. The next term, $\sigma_{x,ij}\Psi_{i+1j}$, is similarly analyzed, and so are the terms $-\Psi_{ij}\sigma_{y,ij+1} + \sigma_{y,ij}\Psi_{ij+1}$ for the case where the hybrid orientation is along y . The last four terms result from hybrid–hybrid orientationally dependent interactions. When the orientation of a hybrid lipid at site ij points along the x (y) axis, the energy is reduced if the nearest neighbor at site $i + 1j$ has the opposite (same) orientation whereas the neighbor at site $ij + 1$ has the same (opposite) orientation. Note that this is captured in eq 8 by the terms $\sigma_{x,ij}\sigma_{x,i+1j} - \sigma_{x,ij}\sigma_{x,ij+1}$ that decrease the energy if σ_x changes sign at every lattice site along i without changing sign along j . The term $\sigma_{y,ij}\sigma_{y,ij+1} - \sigma_{y,ij}\sigma_{y,i+1j}$ is similarly analyzed.

3.2. Isotropic, Homogeneous Membrane with Composition and Orientational Fluctuations. The free energy derived above and described by eq 7 depends on the lattice and is not rotationally invariant. To more closely model experimental systems that have no underlying lattice, it is desirable to work with such a rotationally invariant free energy.

Within the variational approximation used here, the entropic part of the free energy is local and is therefore trivially written as a rotationally invariant expression with no underlying lattice by replacing the lattice sum in eq 11 by an integral over the membrane and replacing A_{ij} by $A(\mathbf{x})$ (A is a composition or orientation field and \mathbf{x} is the position in the membrane). The result is

$$-S = -S_{\text{MF}} - S_{\text{fluct}} \quad (12)$$

where S_{MF} is the mean-field part of the entropy (given by the first three terms in eq 11) and

$$-S_{\text{fluct}} = \frac{1}{a^2} \int d\mathbf{x} \left[\frac{1 - \phi_u^{(0)}}{2\phi_s^{(0)}\phi_h^{(0)}} \delta\phi_s(\mathbf{x})^2 + \frac{1 - \phi_s^{(0)}}{2\phi_u^{(0)}\phi_h^{(0)}} \delta\phi_u(\mathbf{x})^2 + \frac{1}{\phi_h^{(0)}} \delta\phi_s(\mathbf{x})\delta\phi_u(\mathbf{x}) + \frac{1}{\phi_h^{(0)}} |\bar{\sigma}(\mathbf{x})|^2 \right] \quad (13)$$

is the fluctuation part of the entropy. Note that a is a molecular size and is equal to the original lattice spacing, and $\delta\phi_{s(u)}(\mathbf{x})$ is the local saturated (unsaturated) lipid composition fluctuation. Conservation of composition imposes the condition $\delta\phi_h(\mathbf{x}) = -\delta\phi_s(\mathbf{x}) - \delta\phi_u(\mathbf{x})$. Finally, $\bar{\sigma}(\mathbf{x}) = x\hat{\sigma}_x(\mathbf{x}) + y\hat{\sigma}_y(\mathbf{x})$ is the local orientation fluctuation vector.

Section S2 of the Supporting Information shows how the lattice-based expression for the energy part of the free energy (eq 8) can be transformed into one that is a rotationally invariant function of the local deviations of the compositions from their equilibrium values by demanding (1) that all interactions are short-ranged and (2) that they are all expressed in terms of rotationally invariant quantities. Here, we present the final expression for the energy, which is

$$\mathcal{E} = \mathcal{E}_{\text{MF}} + \mathcal{E}_{\text{fluct}} \quad (14)$$

where $\mathcal{E}_{\text{MF}} \propto -2J(\phi_s^{(0)} - \phi_u^{(0)})^2$ is the mean-field part and where

$$\begin{aligned} \mathcal{E}_{\text{fluct}} = & -\frac{2J}{a^4} \int d\mathbf{x} \int d\bar{\Delta} g(\Delta) \{ \Psi(\mathbf{x}) \Psi(\mathbf{x} + \bar{\Delta}) \\ & - \hat{\Delta} \cdot \bar{\sigma}(\mathbf{x}) [\Psi(\mathbf{x} + \bar{\Delta}) - \Psi(\mathbf{x} - \bar{\Delta})] - [\hat{\Delta} \cdot \bar{\sigma}(\mathbf{x})] \\ & \times [\hat{\Delta} \cdot \bar{\sigma}(\mathbf{x} + \bar{\Delta})] + [\hat{\Delta} \times \bar{\sigma}(\mathbf{x})] \cdot [\hat{\Delta} \times \bar{\sigma}(\mathbf{x} + \bar{\Delta})] \} \end{aligned} \quad (15)$$

is the fluctuation part. In this equation, $\Psi(\mathbf{x}) = \delta\phi_s(\mathbf{x}) - \delta\phi_u(\mathbf{x})$ and the function $g(\Delta)$ accounts for the finite range of the interactions. The fact that it depends only on the magnitude of the separation vector between two fields, Δ , ensures rotational invariance. In principle, this provides a way to go beyond nearest-neighbors interactions, but it is sufficient to consider the simple nearest-neighbor situation in which case

$$g_{\text{nn}}(\Delta) = \frac{a}{2\pi} \delta(\Delta - a) \quad (16)$$

where subscript nn stands for nearest neighbors and where Δ and a are scalar quantities. Note that the last two terms inside the integral in eq 15 account for orientation–orientation interactions between hybrid lipids. These are illustrated in Figure 4. Panel A illustrates the term $[\hat{\Delta} \cdot \bar{\sigma}(\mathbf{x})][\hat{\Delta} \cdot \bar{\sigma}(\mathbf{x} + \bar{\Delta})]$ that couples the orientation components parallel to the separation vector between two neighboring hybrids. This contribution to the energy is minimal (negative) if those

components of the orientation fluctuate on the smallest length scale (so that two neighboring lipids have opposite signs for that orientation component). This provides an energetic gain for fluctuations of the orientation. Panel B illustrates the term $-\hat{\Delta} \times \bar{\sigma}(\mathbf{x}) \cdot [\hat{\Delta} \times \bar{\sigma}(\mathbf{x} + \bar{\Delta})]$. This term couples the components of the orientation perpendicular to the separation vector between two neighboring hybrids. This energy term is minimal (negative) when the orientation component is uniform.

To quadratic order in the fluctuations, the free energy that is highly coupled in real space is conveniently written in a Fourier representation where all of the wavevector fluctuation modes decouple. We use the following definition for the Fourier transform,

$$A(\mathbf{k}) = \frac{1}{2\pi} \int d\mathbf{x} e^{-i\mathbf{k} \cdot \mathbf{x}} A(\mathbf{x}) \quad (17)$$

$$\mathbf{M}_{\mathbf{k}} = \begin{pmatrix} T \frac{1 - \phi_u^{(0)}}{2\phi_s^{(0)}\phi_h^{(0)}} - 2J\mathcal{J}_0(ka) & T \frac{1}{2\phi_h^{(0)}} + 2J\mathcal{J}_0(ka) & -i2J \frac{k_x}{k} \mathcal{J}_1(ka) & -i2J \frac{k_y}{k} \mathcal{J}_1(ka) \\ T \frac{1}{2\phi_h^{(0)}} + 2J\mathcal{J}_0(ka) & T \frac{1 - \phi_s^{(0)}}{2\phi_u^{(0)}\phi_h^{(0)}} - 2J\mathcal{J}_0(ka) & i2J \frac{k_x}{k} \mathcal{J}_1(ka) & i2J \frac{k_y}{k} \mathcal{J}_1(ka) \\ i2J \frac{k_x}{k} \mathcal{J}_1(ka) & -i2J \frac{k_y}{k} \mathcal{J}_1(ka) & T \frac{1}{\phi_h^{(0)}} - 2J \frac{k_x^2 - k_y^2}{k^2} \mathcal{J}_2(ka) & -4J \frac{k_x k_y}{k^2} \mathcal{J}_2(ka) \\ i2J \frac{k_y}{k} \mathcal{J}_1(ka) & -i2J \frac{k_x}{k} \mathcal{J}_1(ka) & -4J \frac{k_x k_y}{k^2} \mathcal{J}_2(ka) & T \frac{1}{\phi_h^{(0)}} - 2J \frac{k_y^2 - k_x^2}{k^2} \mathcal{J}_2(ka) \end{pmatrix} \quad (20)$$

where \mathcal{J}_0 , \mathcal{J}_1 , and \mathcal{J}_2 are the zeroth-, first-, and second-order Bessel functions. Equations 18–20 are the main analytical results of this Article. In the next section, we use $\mathcal{F}_{\text{fluct}}$ to predict the composition and orientation fluctuations of the hybrid, saturated, and unsaturated lipids about their equilibrium values in the homogeneous (one-phase) state. We show how hybrid lipids can reduce the characteristic length scales of composition fluctuations in the one-phase regime, analogous to the stabilization of finite domain sizes in the two-phase regime.

4. PREDICTIONS OF THE FLUCTUATIONS AND CORRELATION FUNCTIONS

Before analyzing the composition fluctuations in the single phase, we must determine the conditions under which the system remains macroscopically mixed and does not phase separate or otherwise show modulated phases. These conditions specify the spinodal temperature, T_s , above which all fluctuations (with any wavevector) are locally stable. Given the complexity of the system, the stability analysis presented here (although not equivalent to the more complex, three-component, equilibrium phase diagram) still provides important predictions for the fluctuations, especially for the special case where the spinodal and critical temperatures coincide. Of course, T_s is expected to depend on the overall composition of the membrane. At the spinodal temperature, there is at least one wavevector whose associated composition/orientation fluctuation amplitude can grow with no energy cost. This occurs when

$$\det \mathbf{M}_{\mathbf{k}} = 0 \quad (21)$$

This equation can be solved for T , and the result is a wavevector-dependent temperature $T_{\mathbf{k}}$ at which the fluctuation

with the nearest-neighbor form for g (eq 16) and obtain the following expression for the fluctuation part of the free energy

$$\mathcal{F}_{\text{fluct}} = \frac{1}{a^2} \int d\mathbf{k} \bar{\Psi}_{-\mathbf{k}}^T \mathbf{M}_{\mathbf{k}} \bar{\Psi}_{\mathbf{k}} \quad (18)$$

The free energy also contains a constant mean-field part that we do not report here for simplicity. $\bar{\Psi}_{\mathbf{k}}$ is an array that contains the Fourier components of the composition and orientation fields,

$$\bar{\Psi}_{\mathbf{k}}^T = (\delta\phi_s(\mathbf{k}), \delta\phi_u(\mathbf{k}), \sigma_x(\mathbf{k}), \sigma_y(\mathbf{k})) \quad (19)$$

where the superscript T indicates a transpose and the coupling matrix $\mathbf{M}_{\mathbf{k}}$ is given by

mode $\bar{\Psi}_{\mathbf{k}}$ becomes unstable. The spinodal temperature is the maximum in the set of all wavevector-dependent $T_{\mathbf{k}}$. In other words,

$$T_s = \max[T_{\mathbf{k}}(\phi_d^{(0)}, \phi_h^{(0)})] \quad (22)$$

where

$$T_{\mathbf{k}}(\phi_d^{(0)}, \phi_h^{(0)}) = J \{ 2(1 - \phi_d^{(0)2} - \phi_h^{(0)})\mathcal{J}_0(ka) + \phi_h^{(0)}\mathcal{J}_2(ka) + \left[2(1 - \phi_d^{(0)2} - \phi_h^{(0)})\mathcal{J}_0(ka) - \phi_h^{(0)}\mathcal{J}_2(ka) \right]^2 + 8\phi_h^{(0)}(1 - \phi_d^{(0)2} - \phi_h^{(0)})\mathcal{J}_1(ka)^2 \}^{1/2} \quad (23)$$

and where $\phi_h^{(0)}$ is the average hybrid composition and $\phi_d^{(0)} = \phi_s^{(0)} - \phi_u^{(0)}$ is the difference between the average saturated and unsaturated lipid compositions. Note that $T_{\mathbf{k}}$ depends only on the magnitude of the wavevector \mathbf{k} . This is a consequence of the transformation described above that eliminated any lattice anisotropy and that allows us to describe the rotationally isotropic membranes expected in the single-phase regime.

The left side of Figure 5 plots the spinodal temperature as a function of the fraction of hybrids. There and for the remainder of this Article we will present results for $\phi_d^{(0)} = 0$ (equal fraction of saturated and unsaturated lipids). In that case, the spinodal temperature coincides with the critical temperature and hence eliminates the possibility of first-order transitions. Note that T_s is highly dependent on the composition. The spinodal temperature generally decreases when the amount of hybrid lipid increases, indicating that the presence of hybrids favors the mixing of the saturated and unsaturated lipids. This is in agreement with the experiments in refs 24 and 37, which report that the membrane demixes as the amount of hybrids increases

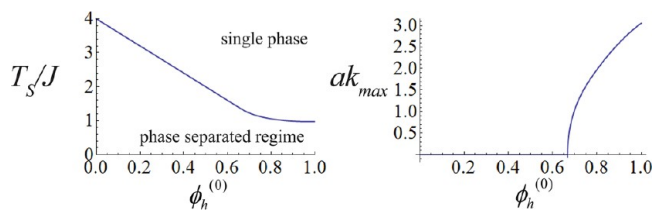


Figure 5. Left panel: The spinodal temperature T_s/J is shown as a function of $\phi_h^{(0)}$ (the overall fraction of hybrid lipids). We have chosen $\phi_d^{(0)} = \phi_s^{(0)} - \phi_u^{(0)} = 0$, a membrane with equal quantities of saturated and unsaturated lipids. The system is in the single phase when $T > T_s$. Note that the spinodal temperature decreases as the amount of hybrid increases, indicating how the hybrid favors the mixing of the saturated and unsaturated lipids. Also, at $\phi_d^{(0)} = 0$ the spinodal temperature coincides with the critical temperature. Right panel: The magnitude of the wavevector that maximizes $T_k(\phi_d^{(0)} = 0, \phi_h^{(0)})$ and determines the spinodal according to eq 22. A Lifshitz line is observed at $\phi_h^{(0)} = 2/3$, above which the first instability is triggered by a nonzero wavevector fluctuation mode.

at constant temperature. Note that our theory predicts that the spinodal temperature shows different dependences on hybrid composition at small and large hybrid fractions. This can be seen in Figure 5 as a slight change in the slope of T_s as a function of $\phi_h^{(0)}$; in the large $\phi_h^{(0)}$ regime, T_s reaches a plateau value. More interesting is the value of the wavevector that shows the first (highest-temperature) instability as the system is cooled from the single phase. That wavevector is denoted by k_{max} in the right panel of Figure 5, which shows that for a small amount of hybrids the instability occurs at $k_{max} = 0$ (indicating macroscopic phase separation). However, as the fraction of hybrids is increased, a crossover regime is reached in which the spinodal temperature is determined by fluctuations with increasingly larger wavevectors whose magnitudes approach $k_{max} = \pi/a$ as $\phi_h^{(0)}$ tends to unity. This should not come as a surprise because, in the case of a system that comprises only hybrid lipids, the energy terms are minimal when the hybrids are arranged in stripes with orientations that change sign over one lattice spacing (so that the wavelength is $2a$). Such striplike structures have also been predicted by earlier models

used to describe other amphiphilic systems.^{49,50} At low enough temperatures, these stripes indeed characterize a modulated phase in which the hybrid orientation varies. At higher temperatures, one expects striplike fluctuations that are not macroscopically correlated but instead have a finite correlation length. The composition at which the dominant fluctuations (peak in the structure factor) have zero wavevector crossover to fluctuations dominated by finite wave vectors is called the Lifshitz line. A simple optimization procedure performed on eq 22 shows that the Lifshitz line is defined by

$$\phi_h^{(0)} = \frac{2}{3}(1 - \phi_d^{(0)2}) \quad (24)$$

Note that for hybrid fractions above the Lifshitz line, Figure 5 indicates that the fluctuation spectrum of the system will have maxima at nonzero wave vectors, something that was first considered by Brazovskii.⁵¹

4.1. Correlation Functions: Fluctuation Domain Sizes (Correlation Length). In the single phase (where all of the lipids are macroscopically mixed), correlation functions describe the local composition fluctuations. In this subsection, we show how the inactant nature of hybrid lipids influences such correlation functions and tends to mix saturated and unsaturated lipids locally. For fluctuations with Gaussian statistics, such as those described by eq 18, any correlation function that contains multiple powers of Ψ (recall that Ψ is an array containing composition and orientation fluctuations as defined by eq 19) can be factored into products of the following pair correlation function matrix,

$$\langle \bar{\Psi}_{-k} \bar{\Psi}_k^T \rangle = \delta_{k+k} \frac{a^2 T}{2} \mathbf{M}_k^{-1} \quad (25)$$

where \mathbf{M}_k^{-1} is the matrix inverse of \mathbf{M}_k . Note that correlation functions in \mathbf{k} space can be directly measured in light, neutron, and/or X-ray scattering experiments. We begin by calculating the saturated lipid autocorrelation function given by

$$C_{ss}(\mathbf{k}) \equiv \langle \delta\phi_s(-\mathbf{k}) \delta\phi_s(\mathbf{k}) \rangle = \frac{a^2 T}{2} [\mathbf{M}_k^{-1}]_{11} \quad (26)$$

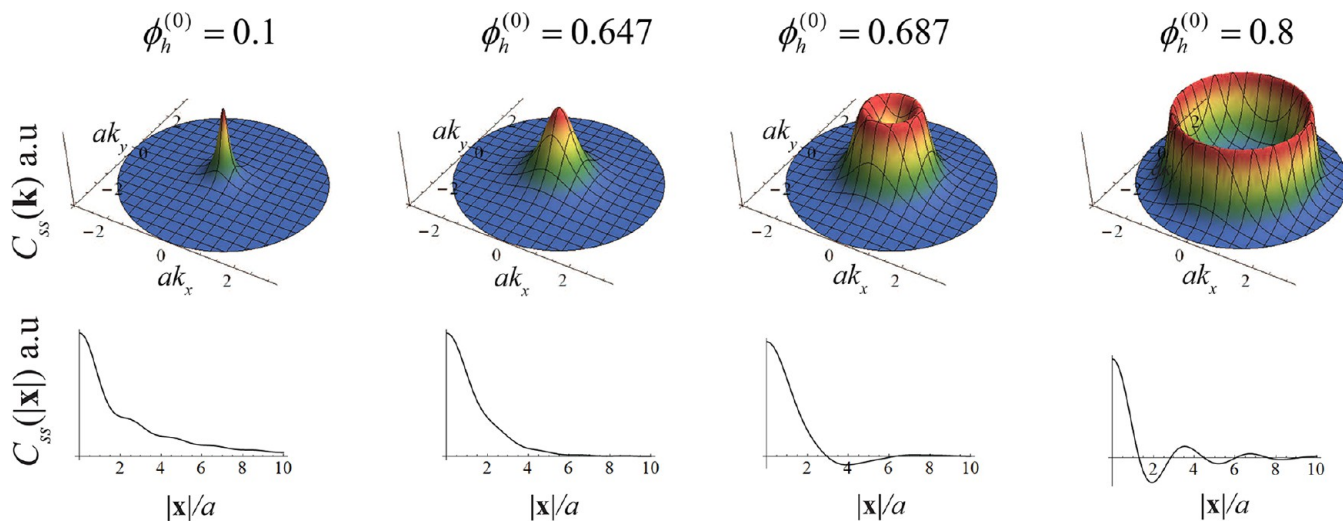


Figure 6. Saturated lipid autocorrelation functions in \mathbf{k} space (top row), $C_{ss}(\mathbf{k}) = \langle \delta\phi_s(-\mathbf{k}) \delta\phi_s(\mathbf{k}) \rangle$, and in real space (bottom row), $C_{ss}(\mathbf{x}) = \langle \delta\phi_s(\mathbf{x}) \delta\phi_s(0) \rangle$, are reported for various membrane compositions at $T = 1.01T_s$ and $\phi_d^{(0)} = \phi_s^{(0)} - \phi_u^{(0)} = 0$. From left to right, $\phi_h^{(0)} = 0.1$, $\phi_h^{(0)} = 0.647$, $\phi_h^{(0)} = 0.687$, and $\phi_h^{(0)} = 0.80$.

where the subscript 11 means that we refer to the 11 part of the inverse of matrix \mathbf{M}_k . This correlation function characterizes the size and shape of saturation-rich composition fluctuations in the single phase.

Figure 6 (top row) shows $C_{ss}(\mathbf{k})$ for four different membrane compositions. In all cases, $\phi_d^{(0)} = 0$ so that $\phi_s^{(0)} = \phi_u^{(0)}$ and the temperature is set 1% above the spinodal (critical) temperature (i.e., $T = 1.01T_s$). For the remainder of the paper, all results will be reported at that temperature. This choice of temperature is arbitrary, but we choose it because it results in correlations that decay slowly enough to be visualized easily. Recall that the spinodal temperature varies with composition and so does the absolute temperature, $T = 1.01T_s$, at which correlation functions are reported. From left to right, the fraction of hybrid lipids is increased as follows: $\phi_h^{(0)} = 0.1$, $\phi_h^{(0)} = 0.647$, $\phi_h^{(0)} = 0.687$, and $\phi_h^{(0)} = 0.8$. Note the significant change in the correlation function that occurs close to the Lifshitz line at $\phi_h^{(0)} = 2/3$ for $\phi_d^{(0)} = 0$. For $\phi_h^{(0)} = 0.647$, the correlation functions is dominated by a broad peak centered at $k_x = k_y = 0$. For $\phi_h^{(0)} = 0.687$, where the hybrid lipid fraction has been increased by only a small amount, a ring-shaped peak is observed whose maximum is at $k_x^2 + k_y^2 = k_{\max}^2$ and where k_{\max} is the magnitude of the wavevector that gives rise to the first unstable fluctuation modes (right panel in Figure 5). At $\phi_h^{(0)} = 0.80$, the \mathbf{k} -space correlation function has a ring shape and peaks at a larger k_{\max} as predicted by Figure 5. The real-space correlations, $C_{ss}(\mathbf{x})$, that correspond to these Fourier modes are shown as 2D plots in the bottom row of Figure 6. The figure was obtained inverting the Fourier transform numerically. Because $C_{ss}(\mathbf{k})$ depends only on the magnitude of \mathbf{k} , $C_{ss}(\mathbf{x})$ depends only on the magnitude of $|\mathbf{x}|$. Note that the correlation function decays on a shorter length scale as the fraction of hybrids is increased from zero to the Lifshitz line ($\phi_h^{(0)} = 2/3$). This indicates that increasing the hybrid fraction provides another way (one way is to increase the temperature) to favor (make more probable) small (nanoscale) fluctuation domains rich in saturated lipids. Above the Lifshitz line, the correlation functions display oscillations whose wavelength decreases as the fraction of hybrids is increased. This illustrates the tendency of hybrid lipids to form striplike fluctuations in the one-phase regime where the interstripe spacing tends toward a molecular size at large hybrid fractions and where many stripes may be located. These are analogous to stable lamellar phases below T_s .

Estimates for the correlation length that is a measure of the length scale of correlated patches rich in saturated lipid can be obtained from the correlation functions in \mathbf{k} -space. Exploiting the fact that $C_{ss}(\mathbf{k})$ is a function of $|\mathbf{k}| = k$ only, we can perform an expansion around the maximum,

$$\begin{aligned} C_{ss}(k) &\approx C_{ss}(k_{\max}) - A(k - k_{\max})^2 \\ &\approx \frac{C_{ss}(k = k_{\max})}{(1 + \xi^2(k - k_{\max})^2)} \end{aligned} \quad (27)$$

where $A = -(\partial^2 C_{ss}(k = k_{\max})/\partial k^2)/2$. This shows that the width of the correlation function in \mathbf{k} space is proportional to $(A/(C_{ss}(k = k_{\max}))) = \xi^2$. That width is related to the spatial decay of the correlation function. Hence, we identify ξ as the correlation length. Figure 7 plots the correlation length as a function of the membrane composition for the same temperature as in Figure 6: $T = 1.01T_s$. Note the very rapid decrease in the length scale of the correlated patches of saturated lipids as the hybrid composition approaches the Lifshitz line. At small

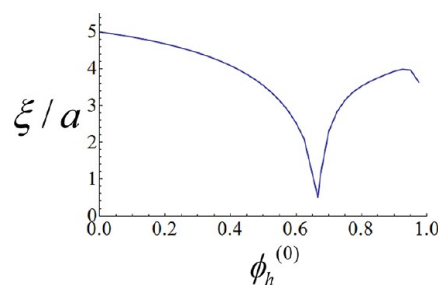


Figure 7. Correlation length associated with the saturated lipid composition fluctuations (see text) shown as a function of the membrane hybrid fraction at $T = 1.01T_s$ and $\phi_d^{(0)} = \phi_s^{(0)} - \phi_u^{(0)} = 0$. Note the sharp decrease as the Lifshitz line is approached.

hybrid compositions, the correlation length decreases almost linearly with the amount of hybrids, and the effect of hybrid lipids is small. This is similar to the results presented earlier by Brewster et al.³³ for a membrane with an infinitely dilute amount of hybrid lipids. In that regime, the behavior of the hybrid lipids is dominated by entropy. Very small fluctuations about the mean hybrid lipid composition are observed, and the fluctuations that are rich in saturated lipids are correlated over large length scales because the interfacial energy between saturated-rich and unsaturated-rich fluctuation domains is reduced by only a small amount because the average hybrid composition is small. As the amount of hybrid lipids is increased, the entropic cost of localizing these lipids at the saturated–unsaturated interfaces is reduced and is also partially offset by attractive hybrid–hybrid orientation interactions. Hybrid lipids can, with some non-negligible probability, adopt conformations that further reduce the interfacial energy between fluctuation domains, leading to a correlation length that decreases in a manner that is stronger than linear with the hybrid fraction. As the amount of hybrids is further increased above the Lifshitz line, the correlation length begins to increase again. This is due to the fact that the hybrids themselves are highly correlated in this high-concentration regime so that the small amounts of saturated lipids in the system show autocorrelations through their coupling with the hybrid lipids.

One crucial prediction of our model is that hybrid lipids favor the spontaneous creation of small-length-scale fluctuation domains (as evidenced by the decreasing correlation lengths) even if the temperature is close to the critical temperature. Reduced correlation lengths close to the Lifshitz line have been observed before by Teubner and Strey,⁵² who postulated a quartic (in powers of k) form for the inverse of the correlation function in terms of three phenomenological parameters to predict the scattering intensity of microemulsions. Of course, exactly at the critical temperature for demixing, the correlation length diverges whether or not hybrids are present. The relationship between the hybrid fraction and the reduction of fluctuation domain sizes (correlation lengths) is one of the main points of this Article. The following subsection focuses on other types of correlation functions and provides information on local fluctuation configurations of saturated, unsaturated, and hybrid lipids in the system. The reader not interested in these details can skip to the discussion.

4.2. Correlation Functions: Hybrid Orientation Fluctuations. We now quantify the orientation fluctuations of the hybrids by examining the xx component of the autocorrelation function of the hybrid lipid orientation vector,

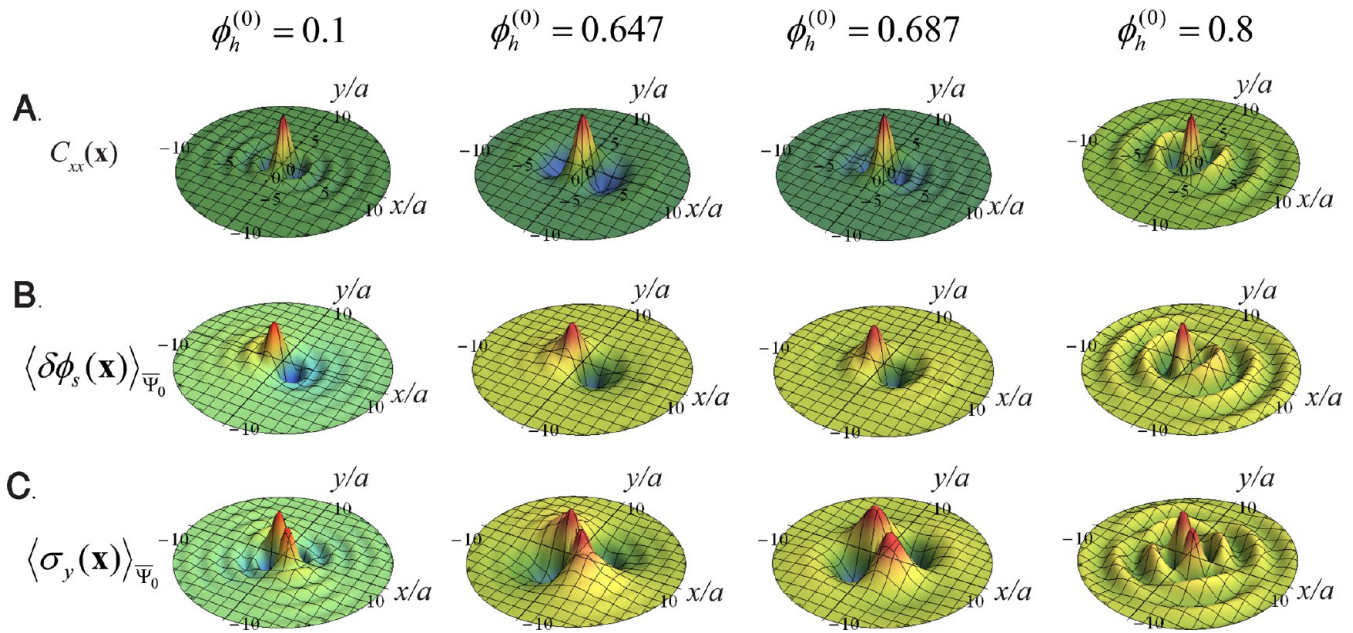


Figure 8. (A) x component of the hybrid lipid orientation autocorrelation function in real space, $C_{xx}(\mathbf{x}) = \langle \sigma_x(\mathbf{x}) \sigma_x(0) \rangle$. Average values of (B) $\delta \phi_s(\mathbf{x})$ and (C) $\sigma_y(\mathbf{x})$ for the case in which the site at $\mathbf{x} = (0, 0)$ is occupied by a hybrid lipid pointing to the right (unsaturated tail to the right $x > 0$, saturated tail to the left $x < 0$); see eq 26 in the main text. From left to right, the membrane composition is $\phi_h^{(0)} = 0.1$, $\phi_h^{(0)} = 0.647$, $\phi_h^{(0)} = 0.687$, and $\phi_h^{(0)} = 0.80$ and $\phi_d^{(0)} = \phi_s^{(0)} - \phi_u^{(0)} = 0$, and the temperature is $T = 1.01T_s$.

$$C_{xx}(\mathbf{k}) \equiv \langle \sigma_x(-\mathbf{k}) \sigma_x(\mathbf{k}) \rangle = \frac{a^2 T}{2} [\mathbf{M}_k^{-1}]_{33} \quad (28)$$

where the subscript 33 means that we refer to the 33 part of the inverse of matrix \mathbf{M}_k . Figure 8 A shows $C_{xx}(\mathbf{x})$ in real space (the Fourier transform has been inverted numerically) for the same compositions as in Figure 6 and for $T = 1.01T_s$. For small amounts of hybrid, many wavevectors contribute to the orientation autocorrelation function, and in real space, the orientations are correlated only at short separations. As the hybrid composition is increased close to the Lifshitz line, the correlation function becomes negative quickly as one proceeds away from the origin along the x -axis and remains anticorrelated at larger separations. In that regime, the hybrid lipids do not form striplike fluctuations where the orientation changes sign. When the hybrid composition is slightly above the Lifshitz line, the correlations display oscillations. Striplike fluctuations are observed, but the oscillation wavelength is not microscopic and the stripes are not correlated over the entire, macroscopic sample. Rather, regions that mix saturated and unsaturated lipids, which favor small wavevector fluctuations, also contain a large amount of hybrids, which favor large wavevector fluctuations. This results in hybrid orientation autocorrelation functions that oscillate with longer wavelengths than they would in the absence of coupling to the saturated-unsaturated fluctuations. The last panel in Figure 8A shows C_{xx} for a large fraction of hybrids. In this case, the orientation fluctuations are highly correlated in the direction along which the hybrid composition oscillates with a wavelength that tends toward the smallest spacing (molecular size) in the system as the hybrid fraction approaches unity. Along the perpendicular direction, no oscillations are observed and the correlation decays on a short length scale for all hybrid fractions.

4.3. Fluctuations in Real Space: Conditional Probabilities. To obtain more insight into the structure of the fluctuations and the cooperative interactions between all types

of lipids, we analyze the fluctuations in real space by calculating several conditional probabilities. The quantity $\langle \Psi(\mathbf{x}) \rangle_{\bar{\Psi}_0}$ is the average value of the fluctuation Ψ at position \mathbf{x} given that the fluctuation at the origin is equal to $\bar{\Psi}_0$. Note that $\bar{\Psi}_0$ is an array whose components specify the deviation of $\phi_s(0)$, $\phi_u(0)$ (and hence $\phi_h(0)$), $\sigma_x(0)$, and $\sigma_y(0)$ from the average values (recall eq 19 that defines $\bar{\Psi}$). Using the fluctuation free energy defined by eq 18, it is simple to show that

$$\langle \Psi(\mathbf{x}) \rangle_{\bar{\Psi}_0} = \frac{1}{2} \int d\mathbf{k} e^{-i\mathbf{k} \cdot \mathbf{x}} \mathbf{M}_k^{-1} \mathbf{G}^{-1} \bar{\Psi}_0 \quad (29)$$

where

$$\mathbf{G} = \frac{1}{2} \int d\mathbf{k} \mathbf{M}_k^{-1} \quad (30)$$

For a membrane with average compositions $\phi_s^{(0)}$ and $\phi_u^{(0)}$, we consider the situation in which the origin is already occupied by a hybrid so that the probability of having saturated and unsaturated lipids is zero there. Furthermore, the orientation of the hybrid at the origin is chosen to point along the x axis (unsaturated tail to the right and saturated tail to the left; $\sigma_x = 1$ and $\sigma_y = 0$). Hence, we set $\bar{\Psi}_0^T = (-\phi_s^{(0)}, -\phi_u^{(0)}, 1, 0)$. The average saturated lipid composition fluctuation, $\langle \delta \phi_s(\mathbf{x}) \rangle_{\bar{\Psi}_0}$ (top row), and the average y component of the hybrid lipid orientation fluctuation, $\langle \sigma_y(\mathbf{x}) \rangle_{\bar{\Psi}_0}$ (bottom row), in the neighborhood of the hybrid at the origin are shown in Figure 8B,C. For a small amount of hybrids, the top row shows that the probability of finding a saturated lipid to the right ($x > 0$) of the reference hybrid is less than the average (mean-field) composition of saturated lipids ($\langle \delta \phi_s(\mathbf{x}) \rangle_{\bar{\Psi}_0} < 0$). To the left ($x < 0$) of the hybrid, that probability is higher than the average fraction of saturated lipids. This behavior is expected because saturated lipids pack more compatibly (have lower energies) when they are adjacent to the saturated tails of hybrid lipids. Note that for small amounts of hybrids the probability of

finding a saturated lipid tends to the average membrane fraction (i.e., $\langle \delta \phi_s(\mathbf{x}) \rangle_{\bar{\Psi}_0} \rightarrow 0$) within a few molecular spacings from the hybrid at the origin.

When the hybrid lipid fraction is increased close to but below the Lifshitz line, the same trends are observed but the spatial decay occurs over a longer range ($\phi_h^{(0)} = 0.647$, in Figure 8B). Just above the Lifshitz line at $\phi_h^{(0)} = 0.687$, $\langle \delta \phi_s(\mathbf{x}) \rangle_{\bar{\Psi}_0}$ displays oscillations. As one proceeds away from the hybrid at the origin, the initial decrease (increase) to the right (left) of the local probability of finding a saturated lipid is followed by an increase (decrease); there is an overshoot before the probability reaches its asymptotic value. For $\phi_h^{(0)} = 0.8$, $\langle \delta \phi_s(\mathbf{x}) \rangle_{\bar{\Psi}_0}$ displays many oscillations. The oscillation period is shorter than for $\phi_h^{(0)} = 0.687$, and the saturated lipid fluctuations remain correlated with the hybrid lipid at the origin over larger distances. Also note that in all panels the value of $\langle \delta \phi_s(\mathbf{x}) \rangle_{\bar{\Psi}_0}$ along $x = 0$ (perpendicular to the orientation of the reference hybrid) is uniform and equal to zero. This means that a hybrid does not bias the local composition toward either saturated or unsaturated lipids in the direction perpendicular to its orientation.

We next examine the conditional probability related to the y components of the hybrid orientation. Figure 8C shows $\langle \sigma_y(\mathbf{x}) \rangle_{\bar{\Psi}_0}$ again for the case in which there is a hybrid at the origin with orientation $\sigma_x = 1$ and $\sigma_y = 0$. For all membrane compositions, the oscillation wavelength and correlation lengths of the orientation correlations are the same as for the composition probabilities, $\langle \phi_s(\mathbf{x}) \rangle_{\bar{\Psi}_0}$. The difference lies in the sign of $\langle \sigma_y(\mathbf{x}) \rangle_{\bar{\Psi}_0}$ in the four quadrants around the hybrid at the origin. In the first quadrant ($x > 0, y > 0$), hybrid lipids in the immediate vicinity of the reference hybrid at the origin preferentially point toward it (in order to minimize the orientation interaction energy given by eq 15). In other words, their σ_x and σ_y components are expected to be negative. Following the same argument, the pattern observed in the other quadrants can be deduced. Note that along the $x = 0$ and $y = 0$ axes, $\langle \sigma_y(\mathbf{x}) \rangle_{\bar{\Psi}_0} = 0$. This means that a hybrid at the origin with $\sigma_x = 1$ and $\sigma_y = 0$ does not bias the σ_y component of a neighboring hybrid lipid in the directions parallel and perpendicular to its orientation.

The behavior along the x direction ($y = 0$ axis) of this conditional probability, Figure 9, further demonstrates how the hybrid, saturated, and unsaturated lipids cooperate to increase the probability of nanoscale-sized fluctuation domains close but below the Lifshitz line and to form striplike fluctuations above the Lifshitz line. Again, we consider a hybrid lipid whose orientation $\sigma_x = 1$ is fixed at the origin. The left panel in the figure is for the case close to but below the Lifshitz line, $\phi_h^{(0)} = 0.647$. It shows an increased local probability of finding an unsaturated lipid in the neighborhood of the origin for $x > 0$. The maximum increase of $\langle \delta \phi_u(\mathbf{x}) \rangle_{\bar{\Psi}_0}$ is attained when $\langle \sigma_x(\mathbf{x}) \rangle_{\bar{\Psi}_0} = 0$. In that region, the local probability of finding a saturated lipid reaches a minimum. Note that the fluctuation region rich in unsaturated lipid to the right of the origin extends over a couple of molecular lengths and is penetrated by regions of correlated orientations of the hybrids. At $\phi_h^{(0)} = 0.8$, the striplike fluctuations are evident. To the right of the hybrid at the origin lies a small fluctuation region rich in unsaturated lipid (and depleted in saturated lipid), followed by a fluctuation region whose orientation is anticorrelated with the hybrid at the

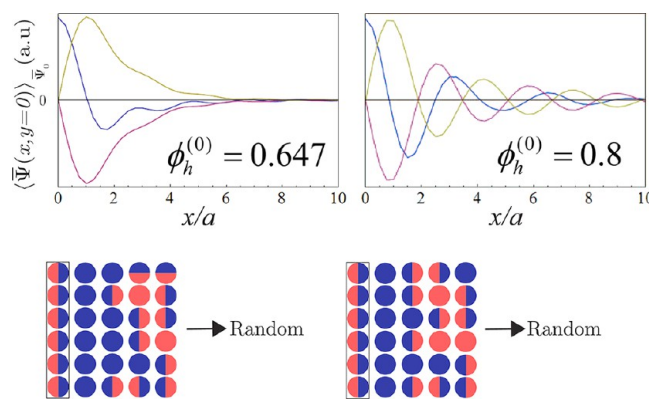


Figure 9. Average value of the x component of the hybrid orientation fluctuation $\sigma_x(x, y = 0)$ (blue line), the average saturated lipid composition fluctuation $\delta \phi_s(x, y = 0)$ (magenta line), and the average unsaturated lipid composition fluctuation $\delta \phi_u(x, y = 0)$ (yellow line) for the case in which the site at $\mathbf{x} = (0, 0)$ is occupied by a hybrid lipid pointing to the right ($\sigma_x = 1$ and $\sigma_y = 0$) as in Figure 8B,C. All curves have been normalized by their maximum value for easier comparison. Left panel: $\phi_h^{(0)} = 0.647$. Right panel: $\phi_h^{(0)} = 0.8$. In both cases, $T = 1.01T_s$. Bottom panels: the lattice model representation is used to sketch how the neighboring lipids may be arranged close to a line of hybrid lipids with the same orientation (in the rectangle). Away from the origin, the configuration becomes random.

origin that is itself followed by a small fluctuation region rich in saturated lipid (depleted in unsaturated lipid). This pattern remains correlated over relatively long distances (compared to the small correlation length observed close to the Lifshitz line) but of course is not macroscopically large in the one-phase region.

5. DISCUSSION

In this Article, we presented a simple model with only one interaction parameter that accounts for the reduction of composition fluctuation domain sizes in saturated–unsaturated–hybrid membranes. A variational theory was used to predict composition fluctuations and correlation functions, thus extending the work of Brewster et al.³³ to the one-phase regime. We show how the correlation lengths characteristic of saturated–unsaturated composition fluctuations are smaller in the presence of the hybrid lipids that have one saturated and one unsaturated chain. When located between a saturated and an unsaturated lipid, the hybrid decreases their packing incompatibility. The model includes the orientation interactions of the hybrid lipids among themselves and extends the previous work of refs 33–35. These orientationally dependent interactions are captured by a lattice model that is a special case of the one proposed by Matsen and Sullivan⁴⁶ to describe the self-assembly of oil/water/amphiphile systems. On one level, our results may be thought of as being more relevant to model membranes than to real cell membranes because the latter contain very few unsaturated lipids and have mostly saturated and hybrid types of lipids. However, we note that real cell membranes contain numerous types of saturated and hybrid lipids with various chain lengths and degrees of unsaturation. One can imagine that two subclasses of hybrid lipids that pack incompatibly could be described by a model similar to the one we proposed, where one class of hybrids effectively behaves as unsaturated lipids relative to the other class that acts as the linactant at the saturated–unsaturated interface. In this sense, some of our results may also be applicable to biological

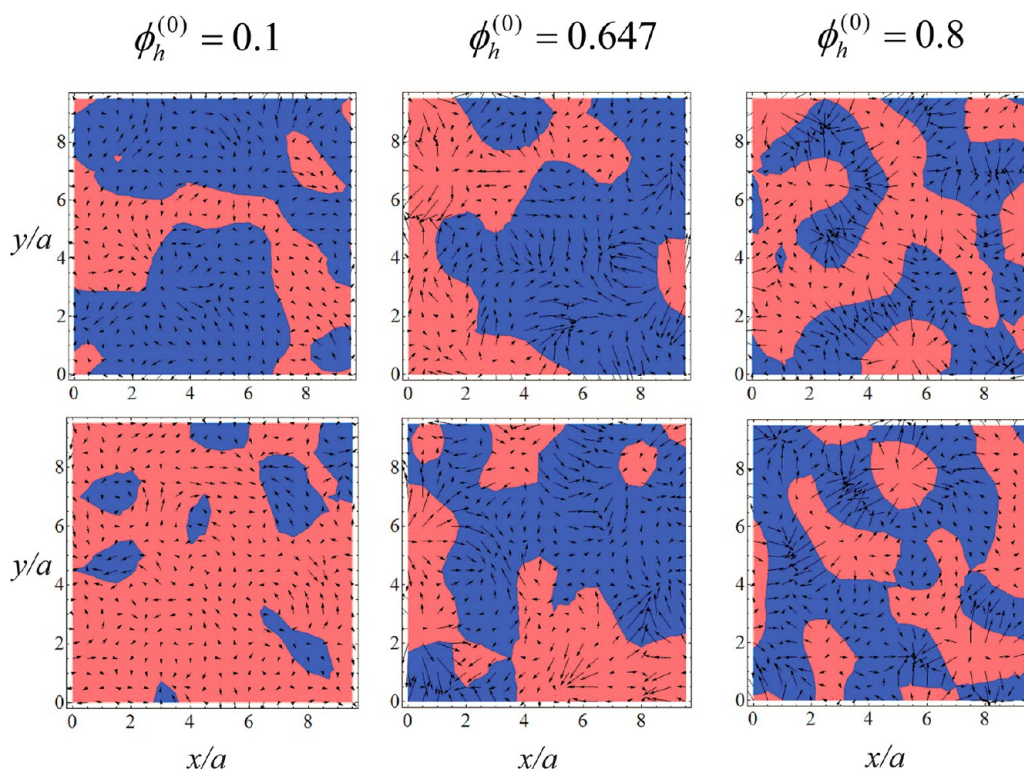


Figure 10. Instantaneous configurations of fluctuations are sampled from eq 18 for $\phi_h^{(0)} = 0.1$ (left panels), $\phi_h^{(0)} = 0.647$ (middle panels), and $\phi_h^{(0)} = 0.8$ (right panels) with $\phi_d^{(0)} = 0$ and $T = 1.01T_s$ in all cases. Thirty wavenumbers along k_x and k_y are uniformly sampled. For each wavenumber, the field $\bar{\Psi}_k$ (eq 19) is determined by choosing random numbers from the Gaussian distribution defined by eq 18. The inverse Fourier transform of $\bar{\Psi}_k$ is obtained numerically, and two instantaneous, real space configurations of saturated lipid fluctuations, $\delta\phi_s(\mathbf{x})$, that are consistent with the predicted correlation functions are shown for the three compositions. Light red represents regions rich in saturated lipids ($\delta\phi_s > 0$), and blue represents a region depleted in saturated lipids ($\delta\phi_s < 0$). The arrows represent the local instantaneous orientation of the hybrid lipid. In our model, configurations near an interface where an arrow points from the light red toward the blue region are energetically favorable. In the middle and right panels, the hybrid lipid indeed adopts such configurations. This is not the case in the left panels ($\phi_h^{(0)} = 0.1$) where large domains rich or depleted in saturated lipids are favored. At $\phi_h^{(0)} = 0.8$ (right panels), local striplike patterns are clearly observed. Note that the interface between the light red and blue region is not sharp; $\delta\phi_s$ varies smoothly from positive to negative values.

membranes, although the details of these various classes of hybrids remain to be identified.

The local system free energy was obtained from a variational principle applied to the lattice model. We then demonstrated how that free energy can be written as a continuous and rotationally invariant theory with no dependence on the underlying lattice in terms of fields that describe the hybrid, saturated, and unsaturated compositions as well as the local hybrid orientation. One advantage of our approach is that it is derived from a microscopic model; the resulting free energy contains only one effective, system-dependent interaction energy whose value can be obtained from measurements of the demixing temperature. Note that our expression for the Fourier representation of the free energy used to predict the fluctuations and correlation functions (eq 18) has a nontrivial wavevector (\mathbf{k}) dependence. If only the leading powers of \mathbf{k} are kept in an expansion for small wave vectors, then the resulting free energy can be written in a manner similar to a Landau–Ginzburg free energy in real space.⁵³ However, in our system this approximation is not very accurate because in some composition ranges the hybrid lipid orientations tend to change sign on a molecular length scale. Hence, high powers of \mathbf{k} are important for membranes with a large fraction of hybrids; we therefore chose to work with the full \mathbf{k} -space expression obtained from the correspondence of our continuum theory with the original lattice model.

The spinodal temperature of the membrane, the temperature above which all fluctuations in the one-phase regime are stable, was predicted from our model. As shown in Figure 5, our model predicts that the spinodal temperature decreases as the amount of hybrids increases. The theory also predicts a Lifshitz line as a function of the hybrid fraction above which the instabilities are triggered by fluctuations with a finite wavevector. The general trend of the hybrids to increase mixing (below the Lifshitz line) has also been observed in recent experiments by Konyakhina et al.²⁴ and by Szekely et al.³⁷ Note that in our analysis the single phase is defined by the fact that the temperature is above the spinodal. This fact guarantees only that we are at temperatures higher than those that result in a continuous transition to phase-separated or modulated regimes. However, discontinuous transitions from the single phase (i.e., first-order transitions) are possible.

Our model free energy was then used to calculate the effects of the hybrid lipid fraction in the membrane on the saturated lipid composition fluctuations in the single phase. These correlation functions are presented here for the case $\phi_d^{(0)} = 0$ (equal fractions of saturated and unsaturated lipids). If we consider the unsaturated lipids in our model, this does not correspond to real cell membranes where $\phi_d^{(0)} \neq 0$ because they contain very small amounts of unsaturated lipids. We chose to present our results for the case of $\phi_d^{(0)} = 0$ because in our model

the spinodal temperature is equal to the critical temperature at that composition.

The two most important predictions of our theory are the following: (1) With increasing amounts of hybrid lipids, the characteristic length scale (correlation length) of saturated and unsaturated-rich fluctuation regions is significantly reduced by intervening regions of correlated hybrid orientation. This is in agreement with earlier studies of amphiphilic systems that predicted shorter correlation length regimes.⁵² The property of the hybrids to reduce the characteristic sizes of the fluctuations is enhanced for the following reasons: (a) There is a finite (and possibly large) amount of hybrids in the system. This reduces the entropic cost associated with the formation of orientationally correlated fluctuation regions. (b) These hybrid regions can reduce the packing incompatibility between neighboring saturated and unsaturated fluctuation regions. The hybrid regions have a finite thickness and can span many molecular lengths. This also reduces the entropic cost of localizing and orienting the hybrids at the saturated–unsaturated interfaces. (c) The interface between neighboring fluctuation regions is diffuse (not molecularly sharp). Neighboring fluctuation regions (saturated hybrid or unsaturated hybrid) can interpenetrate each other. (d) The orientation fluctuations of the hybrids are correlated in a way that is energetically favorable (both with themselves and with the neighboring saturated-/unsaturated-rich fluctuation domains). This point is illustrated in Figure 10 (left and middle panels) which shows two representative snapshots of the configuration of the membrane close to but below the Lifshitz line.

All of these effects lead to reduced correlation lengths of the saturated/unsaturated lipid composition fluctuations even if the temperature is relatively close to the critical temperature. Of course, extremely close to the critical temperature, the correlation lengths diverge; the hybrids therefore renormalize how close one must be to the critical temperature so that fluctuations of a given length scale dominate the system (and can be observed in scattering experiments). The theory predicts a hybrid-based mechanism that explains how composition fluctuations can have correlation lengths in the nanoscale regime even though the system is relatively close to the critical temperature. Note that the experiments of Feigenson and Buboltz²² observed nanoscopic domains in the phase-separated regime of GUVs made of DPPC (Figure 2), DLPC (a saturated lipid with shorter chains), and cholesterol with no hybrid lipids. The hybrid linactant mechanism discussed here is only one of many that can lead to small domains in model membranes. The small domains observed in ref 22 could be due to other effects such as lipid interactions that depend on the nearest-neighbor chain length.

(2) Similar to other theories for amphiphilic systems,^{39,46} our model predicts a Lifshitz line that occurs at large hybrid fractions. Above the Lifshitz line, the theory predicts correlated hybrid regions that can be described as (local and finite-sized) striplike fluctuations of correlated hybrid orientations that alternate with (local and finite-sized) saturated-/unsaturated-rich striplike fluctuation regions. The model explicitly shows how the stripe wavelength decreases with increasing hybrid concentration. At the interface of successive, striplike fluctuation regions, the average hybrid orientation changes sign (e.g., Figure 9). Each striplike region of correlated hybrid orientation is sandwiched between one saturated-rich and one unsaturated-rich striplike fluctuation region. This point is illustrated in Figure 10 (right panels) which shows two

representative “snapshots” (see the caption of Figure 10 for details) of the configuration of the membrane above the Lifshitz line. Local stripes are clearly seen and the correlated hybrid orientations observed in the interfacial region (when the plot changes color) tend to point from the saturated-rich to the unsaturated-rich fluctuation domains. A significant energy gain results from such cooperative correlations. Note that striplike structures have been observed in GUVs that comprise saturated, unsaturated, and hybrid lipids and cholesterol in certain composition ranges. In particular, Figure 2E in Konyakhina et al.²⁴ shows micrometer-scale, striplike modulation. Our model can account for striplike modulations on different length scales (including the scales observed in ref 24) if the hybrid composition is tuned accordingly. Below but close to the Lifshitz line, the tendency of the membrane to form striplike fluctuations competes with the tendency to form large-length-scale composition fluctuations that are precursors of the demixing into two phases that occurs at lower temperatures. This explains why the sizes (correlation lengths) of the saturated/unsaturated fluctuation regions are maximally reduced for large hybrid fractions.

Of course, many of the effects reported in this work are similar to those that are already known to occur in other amphiphilic systems. An extensive amount of theoretical research on such systems was performed in the late 1980s and early 1990s following the pioneer work of Alexander and Widom, who proposed a lattice model to describe microemulsions.^{54,55} These include numerous lattice^{44–46,49} and Landau–Ginzburg^{50,52} models. The key difference of our model is that it is based only on chain–chain interactions and contains only one system-dependent parameter. We have also shown how to recast the lattice model into a continuum and isotropic theory and fully specify the behavior of the system as a function of the fraction of line-active hybrid lipids. As mentioned above, our starting point is a lattice model that is a special case of the one proposed by Matsen and Sullivan.⁴⁶ We also note that those authors obtained an analytical solution of their model using transfer matrix methods.⁵⁶ However, their solution neglects nearest-neighbor hybrid orientation–orientation interactions, which we have shown to be the source of microscopic stripes (i.e., the last two terms in eq 15). Below the Lifshitz line, these interactions increase the stability of the small-length-scale fluctuations (akin to nanodomains) above and beyond the stabilization induced by noninteracting hybrids.

Our prediction of the role of hybrids in stabilizing small correlation lengths (fluctuation regions), summarized in point 1 above, contrasts with the interpretation of Veatch et al.³ that considers standard composition fluctuations in an effectively two-component (saturated/unsaturated) system. This viewpoint attributes the origin of the nanoscale fluctuation regions to the possibility that the cell membrane composition is adjusted so that the physiological temperature (37 °C) is sufficiently above the critical demixing temperature so that the correlation lengths are on the nanoscale. One problem with this approach is that the corresponding nanoscale lifetimes in standard two-component systems are generally rather short compared to what one might imagine to be appropriate for biological relevance. Our fluctuation free-energy model for mixed membranes with hybrid lipids that tend to further “mix” the incompatible saturated and unsaturated species can also be used to predict fluctuation lifetimes. The details of that theory are outside the scope of this Article, but the intuitive idea is that the hybrid lipids allow the predominance of small-length-scale

fluctuations even at temperatures close to the critical point where one normally expects only long-wavelength fluctuations to have large amplitudes. Hence, small-length-scale fluctuations can dominate the fluctuations at temperatures for which the critical slowing down of fluctuations is more significant. That theory shows how the hybrids increase the lifetime associated with finite wavevector fluctuations (relevant to small-length-scale domains) compared to a membrane with no hybrids.⁵⁷

It is useful to compare and distinguish our work from a recently published paper by Hirose, Komura, and Andelman,³⁹ who proposed a phenomenological model free energy and used it to predict composition fluctuations in the single phase of a bilayer made of saturated and hybrid lipids. First, the fluctuation free energy we used is derived from a microscopic model that focuses on chain packing and contains only one parameter that can be obtained from the experimental mixing temperature; this is in contrast to the free energy proposed in ref 39 that is constructed from symmetry arguments and therefore contains many phenomenological parameters. The transformation of our lattice model into a rotationally invariant continuum theory as described above results in a free energy whose terms are similar (they are identical if our free energy, eq 18 is expanded to second order in \mathbf{k}) to those studied in ref 39 but with different coefficients that in our case are fully specified. Second, our microscopic analysis predicts that the interactions associated with the hybrid lipid orientations affect the correlation functions in a qualitative manner; there is a tendency to form striplike fluctuations in the one-phase regime in which the hybrid orientation vector remains correlated over large length scales but changes sign on a molecular length scale in the direction parallel to its orientation vector (and is weakly correlated along the perpendicular direction) at large hybrid fractions. The physics associated with this does not enter into the theory of Hirose et al. for the following reasons: The term in our free energy (eq 15) that favors the stripes is

$$\begin{aligned}\mathcal{E}_{\text{stripe}} &= \frac{2J}{a^4} \int d\mathbf{x} \int d\bar{\Delta} g(\Delta) [\hat{\Delta} \cdot \bar{\sigma}(\mathbf{x})] [\hat{\Delta} \cdot \bar{\sigma}(\mathbf{x} + \bar{\Delta})] \\ &= -\frac{2J}{a^2} \int d\mathbf{k} \{ [\mathbf{k} \cdot \bar{\sigma}_{\mathbf{k}}] [\mathbf{k} \cdot \bar{\sigma}_{-\mathbf{k}}] + \text{other powers of } \mathbf{k} \}\end{aligned}\quad (31)$$

The important point is that the phenomenological theory of Hirose et al. assumed an opposite sign for this term compared to our model in which $J > 0$. Although this has only minor effects on the correlation functions for small amounts of hybrids, it completely changes the nature of the fluctuations for large hybrid fractions because it is this term that favors microscopic striplike fluctuations. Hence, their work does not predict striplike patterns unless their phenomenological parameters have special values that are inconsistent with our microscopic model (i.e., lipid fractions that are larger than 1). The difference comes from the fact that they used an extra level of coarse-graining for the hybrid lipid orientation where averages over a region that is large compared to the molecular size are taken, in contrast to our theory that is derived from a microscopic model. Even after the transformation to the continuum, we keep terms to all orders in the wavevector and do not specialize to the long-wavelength or small-wavevector approximation.

One future objective could be to generalize the model to describe the transition from striplike to compact (i.e., micellar)

domains similar to those observed experimentally in ref 24 (see their Figure 2). In that paper, several types of modulations are observed at rather long length scales. However, nanoscale domains cannot be detected by the microscopy techniques they used that resolve composition differences only on the micrometer scale. Note that these experiments report equilibrium or metastable modulated phases below the demixing temperature. (The modulations are not observed in the one-phase regime.) However, as our theory suggests, precursors of those modulations may still be observed as fluctuations in the single phase. It is possible that the present model may be able to account for fluctuations in the one-phase region that lead to compact domains when the temperature is lowered below the critical temperature if we include the curvature energy associated with the hybrids as proposed by Brewster et al.⁵⁸ This energy also originated in the chain packing interactions and is related to the fact that the area projected on the plane defined by the membrane of the unsaturated tail of a hybrid lipid is larger than that of the saturated tail. In the snapshot reported in Figure 10, this would favor contours that curve in a way such that the saturated-rich domains (light red) are on the convex side. In general, this means that the bending part of the free energy should include the effects of spontaneous curvature.^{59,60}

■ ASSOCIATED CONTENT

§ Supporting Information

Technical details on the variational principle used in section 3.1 and on the procedure to obtain an isotropic and continuous description of the membrane from the lattice as mentioned in section 3.2. This material is available free of charge via the Internet at <http://pubs.acs.org>.

■ AUTHOR INFORMATION

Corresponding Author

*E-mail: sam.safran@weizmann.ac.il

Notes

The authors declare no competing financial interest.

■ ACKNOWLEDGMENTS

We are grateful for discussions with Michael Schick, David Andelman, Shigeyuki Komura, Gerald Feigenson, James Sethna, Lia Addadi, Sarah Keller, Phil Pincus, Tetsuya Yamamoto, Benjamin Machta, Sarah Veatch, Richard Vink, Uri Raviv, Martin Grant, and Nir Gov. The Israel Science Foundation, the Schmidt Minerva Center, and the historic generosity of the Perlman Family Foundation are gratefully acknowledged for funding this research. B.P. is grateful to the Azrieli Foundation for the award of an Azrieli Fellowship.

■ REFERENCES

- (1) Boal, D. *Mechanics of the Cell*; Cambridge University Press: Cambridge, 2002.
- (2) Feigenson, G. W. Phase behavior of lipid mixtures. *Nat. Chem. Biol.* **2006**, *2*, 560.
- (3) Veatch, S.; Cicuta, P.; Sengupta, P.; Honerkamp-Smith, A.; Holowka, D.; Baird, B. Critical fluctuations in plasma membrane vesicles. *ACS Chem. Biol.* **2008**, *5*, 287.
- (4) Mayor, S.; Rao, M. Rafts: scale-dependent, active lipid organization at the cell surface. *Traffic* **2004**, *5*, 231.
- (5) Hancock, J.; Parton, R. Ras plasma membrane signalling platforms. *Biochem. J.* **2005**, *389*, 1.

- (6) Suzuki, K.; Fujiwara, T.; Sanematsu, F.; Iino, R.; Edidin, M.; Kusumi, A. GPI-anchored receptor clusters transiently recruit Lyn and G alpha for temporary cluster immobilization and Lyn activation: single-molecule tracking study 1. *J. Cell. Biol.* **2007**, *177*, 717.
- (7) Chiang, S.; Baumann, C.; Kanzaki, M.; Thurmond, D.; Watson, R.; Neudauer, C.; Macara, I.; Pessin, J.; Saltiel, A. Insulin-stimulated GLUT4 translocation requires the CAP-dependent activation of TC10. *Nature* **2001**, *410*, 944.
- (8) Suzuki, N.; Suzuki, S.; Millar, D. G.; Unno, M.; Hara, H.; Calzascia, T.; Yamasaki, S.; Yokosuka, T.; Chen, N.-J.; Elford, A. R.; Suzuki, J.-i.; Takeuchi, A.; Mirtsos, C.; Bouchard, D.; Ohashi, P. S.; Yeh, W.-C.; Saito, T. A critical role for the innate immune signaling molecule IRAK-4 in T cell activation. *Science* **2006**, *311*, 1927.
- (9) Palazzo, A.; Eng, C.; Schlaepfer, D.; Marcantonio, E.; Gundersen, G. Localized stabilization of microtubules by integrin- and FAK-facilitated rho signaling. *Science* **2004**, *303*, 836.
- (10) Hancock, J. Lipid rafts: contentious only from simplistic standpoints. *Nat. Rev. Mol. Cell Biol.* **2006**, *7*, 456.
- (11) Elson, E.; Fried, E.; Delbow, J.; Genin, G. Phase separation in biological membranes: integration of theory and experiment. *Annu. Rev. Biophys.* **2010**, *39*, 207.
- (12) Machta, B.; Papanikolaou, S.; Sethna, J.; Veatch, S. Minimal model of plasma membrane heterogeneity requires coupling cortical actin to criticality. *Biophys. J.* **2011**, *100*, 1668.
- (13) Speck, T.; Vink, R. Random pinning limits the size of membrane adhesion domains. *Phys. Rev. E* **2012**, *86*, 031923.
- (14) Schick, M. Membrane heterogeneity: manifestation of a curvature-induced microemulsion. *Phys. Rev. E* **2012**, *85*, 031902.
- (15) Krobath, H.; Rózycki, B.; Lipowsky, R.; Weikl, T. Line tension and stability of domains in cell-adhesion zones mediated by long and short receptor-ligand complexes. *PLoS One* **2011**, *6*, e23284.
- (16) Yethiraj, A.; Weisshaar, J. Why are lipid rafts not observed in vivo? *Biophys. J.* **2007**, *93*, 3113.
- (17) Fischer, T.; Vink, R. Domain formation in membranes with quenched protein obstacles: lateral heterogeneity and the connection to universality classes. *J. Chem. Phys.* **2011**, *134*, 055106.
- (18) Almeida, P.; Beast, A.; Hinderliter, A. Monte Carlo simulation of protein-induced lipid demixing in a membrane with interactions derived from experiment. *Biophys. J.* **2011**, *101*, 1930.
- (19) Dietrich, C.; Bagatolli, L.; Volovyk, Z.; Thompson, N.; Levi, M.; Jacobson, K.; Gratton, E. Lipid Rafts Reconstituted in Model Membranes. *Biophys. J.* **2001**, *80*, 1417.
- (20) Samsonov, A. V.; Mihalyov, I.; Cohen, F. S. Characterization of cholesterol-sphingomyelin domains and their dynamics in bilayer membranes. *Biophys. J.* **2001**, *81*, 1486.
- (21) Veatch, S. L.; Keller, S. L. Organization in lipid membranes containing cholesterol. *Phys. Rev. Lett.* **2002**, *1417*.
- (22) Feigenson, G. W.; Buboltz, J. Ternary phase diagram of dipalmitoyl-PC/dilauroyl-PC/cholesterol: nanoscopic domain formation driven by cholesterol. *Biophys. J.* **2001**, *80*, 2775.
- (23) Heberle, F.; Wu, J.; Goh, S.; Petruzielo, R.; Feigenson, G. Comparison of three ternary lipid bilayer mixtures: FRET and ESR reveal nanodomains. *Biophys. J.* **2010**, *99*, 3309.
- (24) Konyakhina, T.; Goh, S.; Amazon, J.; Heberle, F.; Wu, J.; Feigenson, G. Control of a nanoscopic-to-macroscopic transition: modulated phases in four-component DSPC/DOPC/POPC/Chol giant unilamellar vesicles. *Biophys. J.* **2011**, *101*, L08.
- (25) van den Bogaart, G.; Meyenberg, K.; Risselada, H.; Amin, H.; Willig, K.; Hubrich, B.; Dier, M.; Hell, S.; Grubmüller, H.; Diederichsen, U.; Jahn, R. Membrane protein sequestering by ionic protein–lipid interactions. *Nature* **2011**, *479*, 552.
- (26) Levantal, I.; Grzybek, M.; Simons, K. Raft domains of variable properties and compositions in plasma membrane vesicles. *Proc. Natl. Acad. Sci. U.S.A.* **2011**, *108*, 11411.
- (27) Svetlovics, J.; Wheaton, S.; Almeida, P. Phase separation and fluctuations in mixtures of a saturated and an unsaturated phospholipid. *Biophys. J.* **2012**, *102*, 2526.
- (28) Wolff, J.; Marques, C.; Thalmann, F. Thermodynamic approach to phase coexistence in ternary phospholipid-cholesterol mixtures. *Phys. Rev. Lett.* **2011**, *106*, 128104.
- (29) Putzel, G. G.; Schick, M. Phenomenological model and phase behavior of saturated and unsaturated lipids and cholesterol. *Biophys. J.* **2008**, *95*, 4756.
- (30) Putzel, G.; Schick, M. Insights on raft behavior from minimal phenomenological models. *J. Phys.: Condens. Matter* **2011**, *23*, 284101.
- (31) Honerkamp-Smith, A.; Veatch, S.; Keller, S. An introduction to critical points for biophysicists; observations of compositional heterogeneity in lipid membranes. *Biochim. Biophys. Acta* **2009**, *1788*, 53.
- (32) Sriram, I.; Schwartz, D. Line tension between coexisting phases in monolayers and bilayers of amphiphilic molecules. *Surf. Sci. Rep.* **2012**, *67*, 143.
- (33) Brewster, R.; Pincus, P.; Safran, S. Hybrid lipids as a biological surface-active component. *Biophys. J.* **2009**, *97*, 1087.
- (34) Yamamoto, T.; Brewster, R.; Safran, S. Chain ordering of hybrid lipids can stabilize domains in saturated/hybrid/cholesterol lipid membranes. *Europhys. Lett.* **2010**, *91*, 28002.
- (35) Yamamoto, T.; Safran, S. Line tension between domains in multicomponent membranes is sensitive to degree of unsaturation of hybrid lipids. *Soft Matter* **2011**, *7*, 7021.
- (36) Schafer, L.; Marrink, S. Partitioning of lipids at domain boundaries in model membranes. *Biophys. J.* **2010**, *99*, L91.
- (37) Szekeley, O.; Schilt, Y.; Steiner, A.; Raviv, U. Regulating the size and stabilization of lipid raft-like domains and using calcium ions as their probe. *Langmuir* **2011**, *27*, 14767.
- (38) Chen, K.; Jayaprakash, C.; Pandit, R.; Wenzel, W. Microemulsions - a Landau-Ginzburg theory. *Phys. Rev. Lett.* **1990**, *65*, 2736.
- (39) Hirose, Y.; Komura, S.; Andelman, D. Concentration fluctuations and phase transitions in coupled modulated bilayers. *Phys. Rev. E* **2012**, *86*, 021916.
- (40) Chiantia, S.; London, E. Acyl chain length and saturation modulate interleaflet coupling in asymmetric bilayers: effects on dynamics and structural order. *Biophys. J.* **2012**, *103*, 2311.
- (41) Kumar, P. B. S.; Gompper, G.; Lipowsky, R. Modulated phases in multicomponent fluid membranes. *Phys. Rev. E* **1999**, *60*, 4610.
- (42) Lee, D. W.; Min, Y.; Dhar, P.; Ramachandran, A.; Israelachvili, J.; Zasadzinski, J. Relating domain size distribution to line tension and molecular dipole density in model cytoplasmic myelin lipid monolayers. *Prod. Natl. Acad. Sci. U.S.A.* **2011**, *108*, 9425.
- (43) Mercado, F. V.; Maggio, B.; Wilke, N. Modulation of the domain topography of biphasic monolayers of stearic acid and dimyristoyl phosphatidylcholine. *Chem. Phys. Lipids* **2012**, *165*, 232.
- (44) Gompper, G.; Schick, M. Phase and scattering behavior of disordered aqueous surfactant solutions as the binary limit of ternary microemulsions. *Chem. Phys. Lett.* **1989**, *163*, 475.
- (45) Gompper, G.; Schick, M. *Self-Assembling Amphiphilic Systems*; Academic Press: London, 1994.
- (46) Matsen, M.; Sullivan, D. Lattice model for surfactants in solution. *Phys. Rev. A* **1990**, *41*, 2021.
- (47) Elliott, R.; Szleifer, I.; Schick, M. Phase diagram of a ternary mixture of cholesterol and saturated and unsaturated lipids calculated from a microscopic model. *Phys. Rev. Lett.* **2006**, *96*, 098101.
- (48) Safran, S. *Statistical Thermodynamics of Surfaces, Interfaces and Membranes*; Westview Press: Boulder, CO, 2003.
- (49) Dawson, K. Interfaces between phases in a lattice model of microemulsions. *Phys. Rev. A* **1987**, *35*, 1766.
- (50) Gompper, G.; Schick, M. Correlation between structural and interfacial properties of amphiphilic systems. *Phys. Rev. Lett.* **1990**, *65*, 1116.
- (51) Brazovskii, S. Phase transition of an isotropic system to a nonuniform state. *Sov. Phys. JETP* **1975**, *41*, 85.
- (52) Teubner, M.; Strey, R. Origin of the scattering peak in microemulsions. *J. Chem. Phys.* **1987**, *87*, 3195.
- (53) Ginzburg, V.; Landau, L. On the theory of superconductivity. *Zh. Eksp. Teor. Fiz.* **1950**, *20*, 1064.

- (54) Alexander, S. Lattice gas model for microemulsions. *J. Phys., Lett.* **1978**, 39, L1.
- (55) Widom, B. Lattice model of microemulsions. *J. Chem. Phys.* **1986**, 84, 6943.
- (56) Matsen, M.; Sullivan, D. Lattice model for microemulsions in 2 dimensions. *Phys. Rev. A* **1992**, 46, 1985.
- (57) Palmieri, B.; Safran, S. A. To be submitted for publication.
- (58) Brewster, R.; Safran, S. Line active hybrid lipids determine domain size in phase separation of saturated and unsaturated lipids. *Biophys. J.* **2010**, 98, L21.
- (59) Helfrich, W. Elastic properties of lipid bilayers-theory and possible experiments. *Z. Naturforsch. C* **1973**, 28, 693.
- (60) Safran, S. Curvature elasticity of thin films. *Adv. Phys.* **1999**, 48, 395.